Applied Combustion Technology, Inc.

Applied Combustion Technology, Inc.

ACT
APPLIED COMBUSTION
TECHNOLOGY, INC.
2910 N. ORANGE AVENUE
ORLANDO, FLORIDA 32804
(305) 894-2910

FINAL REPORT

on

Expanded Ignition Effectiveness Tests of Selected Igniter Materials with Navy Propellants

Contract No. N00174-81-C-0453

Performance Period

October 1981 - September 1982

Submitted to

Gun Systems Engineering
Naval Ordnance Station
Indian Head, MD 20640

Submitted by

A. Michael Varney and John Martino
Applied Combustion Technology, Inc.
2910 N. Orange Avenue
Orlando, FL 32804

ACT-TR-8136

8-16-82

REPORT DOCUMENTATION PAGE

READ INSTRUCTIONS BEFORE COMPLETING FORM

1. REPORT NUMBER ACT-TR-8136	2. GOVT ACCESSION NO. AD-A120790	3. RECIPIENT'S CATALOG NUMBER
4. TITLE (and Subtitle) Expanded Ignition Effectiveness Tests of Selected Igniter Materials with Navy Propellants		5. TYPE OF REPORT & PERIOD COVERED Final Report October 1981-Sept. 1982
		6. PERFORMING ORG. REPORT NUMBER ACT-TR-8136
7. AUTHOR(s) Varney, A. Michael and Martino, John		8. CONTRACT OR GRANT NUMBER(s) N00174-81-C-0453
9. PERFORMING ORGANIZATION NAME AND ADDRESS Applied Combustion Technology, Inc. 2910 N. Orange Avenue Orlando, FL 32804		10. PROGRAM ELEMENT, PROJECT, TASK AREA & WORK UNIT NUMBERS
11. CONTROLLING OFFICE NAME AND ADDRESS Gun Systems Engineering Naval Ordnance Station Indian Head, MD 20640		12. REPORT DATE September 1982
		13. NUMBER OF PAGES 41
14. MONITORING AGENCY NAME & ADDRESS(if different from Controlling Office)		15. SECURITY CLASS. (of this report) Unclassified
		15a. DECLASSIFICATION/DOWNGRADING SCHEDULE

16. DISTRIBUTION STATEMENT (of this Report)

Distribution Unlimited.

17. DISTRIBUTION STATEMENT (of the abstract entered in Block 20, if different from Report)

18. SUPPLEMENTARY NOTES

19. KEY WORDS (Continue on reverse side if necessary and identify by block number)

NACO Propellant	Black Powder	Ignition Effectiveness
NOSOL-318 Propellant	Boron Potassium Nitrate	
NOSOL-363 Propellant	Magnesium-teflon-viton	
LOVA Propellant	Nitrocellulose	
Igniter Energy	Boron molybdenum trioxide	

20. ABSTRACT (Continue on reverse side if necessary and identify by block number)

Diagnostic ignition experiments have been conducted using a high-pressure flow through combustor to evaluate the ignition effectiveness of black powder, boron potassium nitrate, magnesium-teflon-viton, nitrocellulose, and boron molybdenum trioxide with four propellants--NACO, NOSOL-318, NOSOL-363 and LOVA. Over 250 experiments have been conducted to determine the ability of various igniter materials to ignite gun

20. propellants beyond the immediate vicinity of the gun igniter--that is, after filtering through and being cooled by an inert propellant simulant zone positioned between the igniter and the live propellant. The ignition effectiveness has been determined quantitatively by the amount of igniter thermal energy, based on its heat of explosion, required to ignite a propellant 50 percent of the time. Analyses and results are given which present the relative effectiveness of the igniter materials in terms of the different ignition stimuli (e.g., gases, liquids, and solids ratios).

PREFACE

This report summarizes project analyses and results for the experimental documentation of the ignition effectiveness of BP, $BKNO_3$, NC, MTV, and $BMoO_3$ igniter materials with NACO, NOSOL-318, NOSOL-363, and LOVA propellants. The experimental program was conducted under Contract N00174-81-C-0453 for the Naval Ordnance Station, Indian Head, Maryland from October 1981 to September 1982 by Applied Combustion Technology, Inc., Orlando, Florida. Mr. Charles Irish served as technical monitor for NOSIH and Dr. Michael Varney served as Principal Investigator for Applied Combustion Technology, Inc.

TABLE OF CONTENTS

LIST OF FIGURES

LIST OF TABLES

1.0 INTRODUCTION

1.1 Background

Applied Combustion Technology, Inc. has been involved in research to further understand the ignition effectiveness of various igniter materials with U. S. Navy propellants. As part of this ongoing research, Applied Combustion Technology, Inc. has designed, fabricated, and developed an ignition energetics characterization device (IECD) capable of conducting controlled ignition experiments under simulated gun conditions. The results presented herein document the ignition effectiveness of black powder (BP), boron potassium nitrate ($BKNO_3$), IMR 4895 (NC), magnesium teflon-viton (MTV), and boron molybdenum trioxide ($BMoO_3$) with NACO, NOSOL-318, NOSOL-363, and LOVA propellants.

1.2 Project Objectives

In order to quantitize the ignition effectiveness of an igniter material, it is desirable to establish both the total energy deposition and the rate of energy deposition required to produce a sustained ignition in a live propellant bed. The primary objective of the current project was to use the igniter system developed under the initial phase of Contract N00174-80-C-0138 and conduct a series of diagnostic experiments to investigate the ignitibility of NACO, NOSOL-318, NOSOL-363, and LOVA propellants when subjected to different ignition stimuli (e.g., hot gases, liquids, solids) as represented by BP, $BKNO_3$, NC, MTV, and $BMoO_3$ igniter materials.

1.3 Achievements

During the current project, Applied Combustion Technology, Inc. has achieved the following goals:

1. Conducted 278 ignition effectiveness tests with NACO, NOSOL-318, and NOSOL-363 using BP, $BKNO_3$, NC, MTV, and $BMoO_3$ igniter materials.
2. Conducted Bruceton sensitivity analyses for seventeen (17) series of ignition effectiveness test data.
3. Developed an analytical model describing the igniter performance in terms of experimentally measured pressure-time data.
4. Performed relative rankings of all igniter materials and identified plausible ignition stimuli modes for each material.

Ignition effectiveness tests were conducted using the Ignition Energetics Characterization Device (Ref. 1) with a fixed zone of inert propellant simulant separating the igniter vent exit plane and the live propellant zone. Calculated igniter performance criteria suggest that the effective stimuli for each igniter material are:

Overall Calculated Ranking	Material	Effective Stimuli
1 (Best)	MTV	Liquids
2	$BKNO_3$	Gases, vapors, and solids
3	BP	Liquids
4 (Worst)	NC	Gases

The calculated rankings and the experimentally determined rankings based upon 50 percent firepoint energy levels are given on the next page:

Overall Ranking	Calculated Ranking	50% Firepoint Ranking
1 (Best	MTV	BP
2	$BKNO_3$	$BKNO_3$
3	BP	MTV
4 (Worst)	NC	NC

Comparisons between calculated results and the experimentally determined results are presented herein with supporting test data, analyses, and conclusions.

2.0 EXPERIMENTAL

2.1 IECD Hardware Description

The IECD hardware, Figure 2.1, consists of five functional elements, listed below:

1. Igniter Assembly. The igniter assembly consists of an end closure cap machined to accept an electrically initiated primer and a variety of different igniter configurations, including axial vent (shown), radial vent, and bayonet type systems.
2. Combustion Chamber. The combustion chamber is made from aircraft grade E-4340 steel, hardened to a minimum yield strength of 200 ksi. The nominal chamber volume is 1945 cc minus the volume of the igniter vent assembly, and is equipped with six (6) access ports to monitor pressure and/or light generation response during ignition and flame spreading.
3. Mixing Chamber. The mixing chamber is connected to the combustion chamber via a control nozzle (variable in size and replaceable) and serves the function of mixing the combustion gases exiting from the combustion chamber as well as controlling the combustion chamber p-t profile.
4. Auxiliary Test Chamber. The auxiliary test chamber is a combustion gas diagnostic section designed to permit determination of the composition and enthalpy level of the gases exiting the propellant bed.

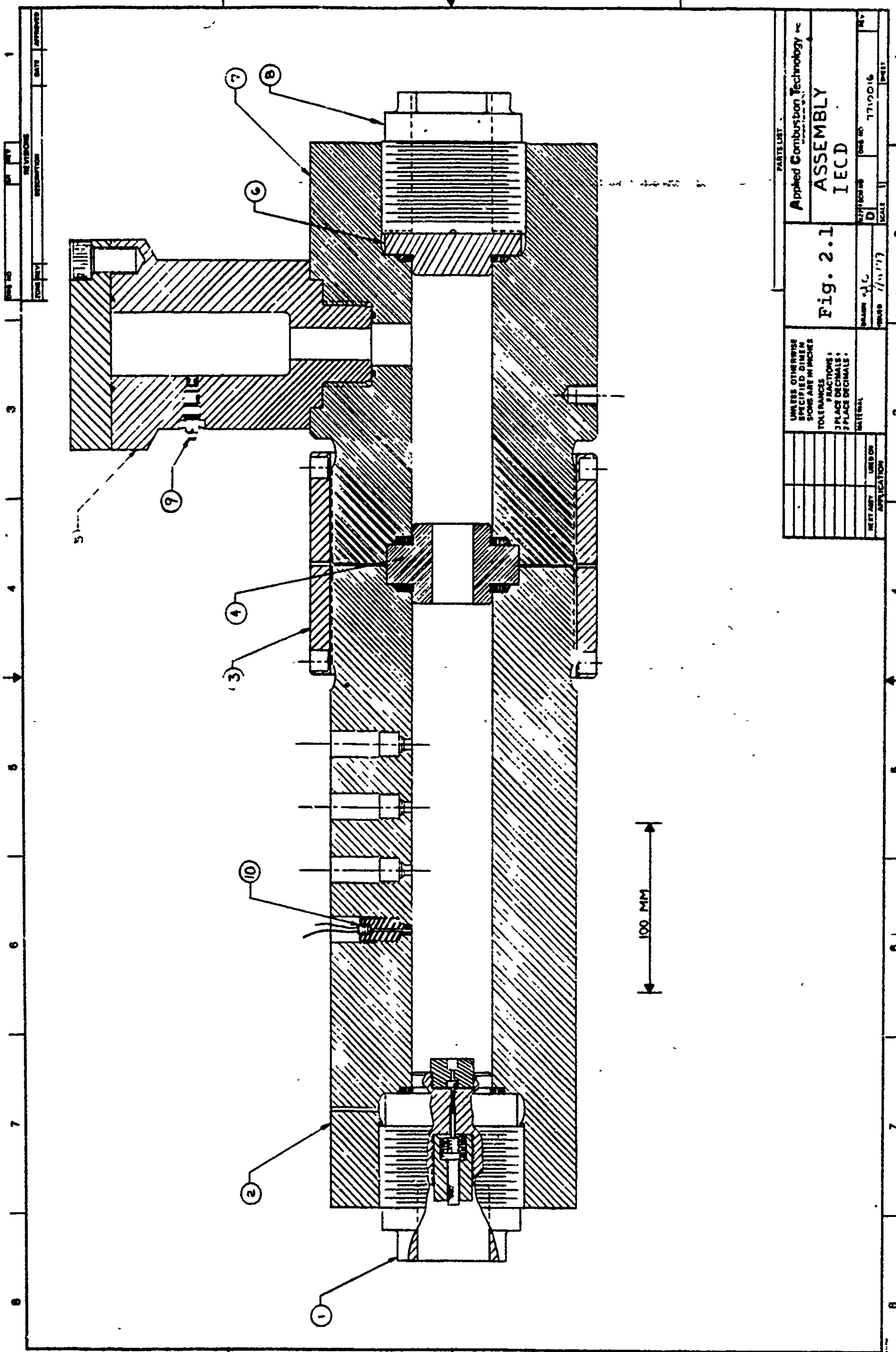
Applied Combustion Technology Inc
PARTS LIST
ASSEMBLY
IECD
Fig. 2.1
100 MM
1
2
3
4
6
7
8
9
10
UNLESS OTHERWISE SPECIFIED DIMENSIONS ARE IN INCHES
TOLERANCES
FRACTIONS
MATERIAL
NEXT ASSY
USED ON
APPLICATION
REVISIONS
DESCRIPTION
DATE
APPROVED

5. Blowdown Nozzle. The blowdown nozzle permits venting of the entire system and is installed with a burst diaphragm or a constant area bleed vent.

The igniter system, Figure 2.2, is designed to provide overall event sequencing for data acquisition while facilitating some general design variations which can be easily achieved without extensive rework during the igniter testing and development. Toward this objective, an Olin Corporation M52A3B1 electric primer was chosen as the base element in the ignition train. To provide some flexibility in choice of igniter materials, an axial vent igniter with a cavity volume of 1 in^3 (16.39 cc) was designed with provisions for up to 5 axial vents. Individual vents consist of a No. 10-32 tapped hole in the velocity control element, each of which can be fitted with a pre-drilled (or blank) Allen-head set screw. This technique permits the easy variation of vent diameter from test to test and/or the replacement of eroded vents. The center vent has been oversized to accept a PCB-111A (10,000 psi) transducer to permit primer calibration and primer/igniter coupling calibration.

2.2 Experimental Procedures

2.2.1 Igniter Calibration Tests

Pressure profiles for the primer and the various igniter materials were acquired for calibration and data correlation. Primary control variables available for the igniter calibration tests consisted of:

1. Axial vent variations in outflow area
2. Igniter material type
3. Igniter material quantity

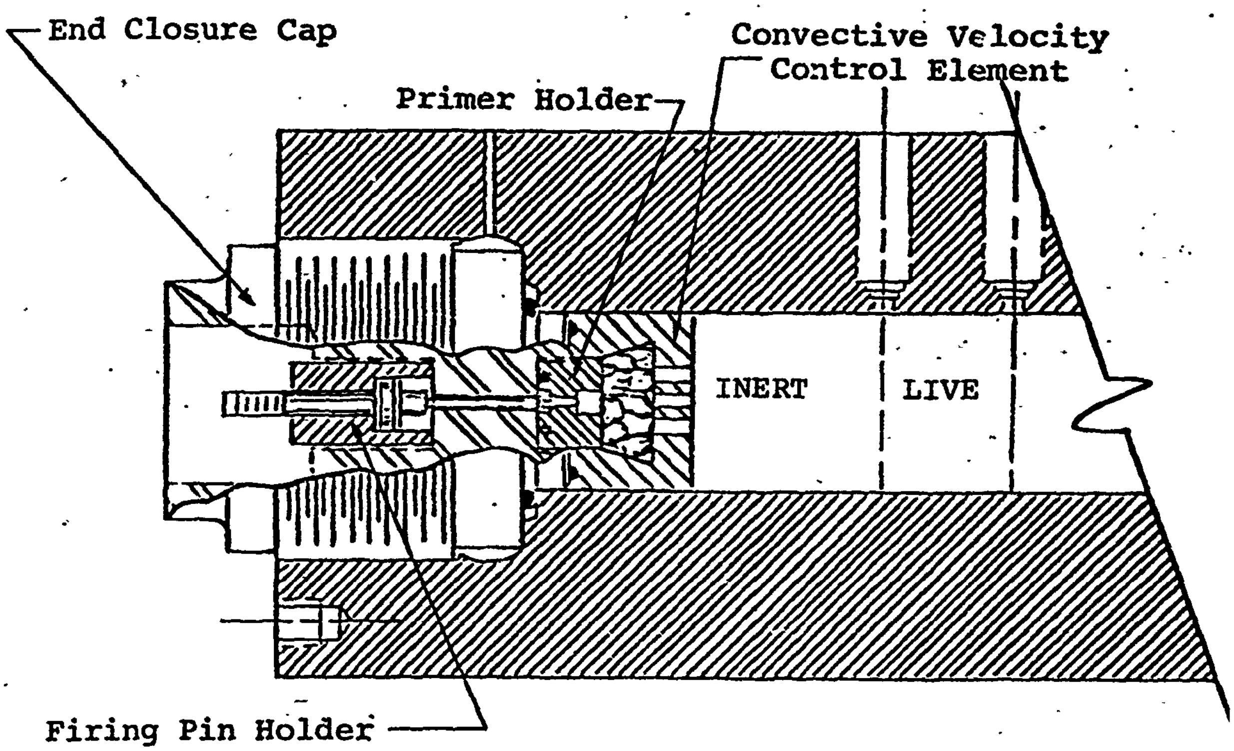

Figure 2.2 Igniter Assembly

Axial vent outflow variations were achieved by selecting the outflow orifice size desired for up to five outflow elements. This type of variation permits control over the output velocity and mass flow delivered to the propellant bed. The igniter materials used in the test series consisted of commercially available black powder (Goex, Inc.), $BKNO_3$ pellets, $BKNO_3$ granules, NC (IMR 4895), MTV, and $BMoO_3$. Initial tests included calibration of the primer-only and the igniter system yielding pressure time profiles, as typically shown in Figure 2.3, obtained by installing a pressure transducer in the centerline vent location. Each primer function pressure-time record, Figure 2.3a, was analyzed for:

1. Ignition delay time referenced with respect to event signal initiation
2. Pressurization rate
3. Peak pressure
4. Time to reach peak pressure
5. Overall event duration.

Each ignition function test, Figure 2.3b, was analyzed for:

1. Primer peak pressure
2. Igniter material ignition pressure
3. Igniter material pressurization rate
4. Peak igniter pressure
5. Time to reach peak igniter pressure
6. Event duration.

Using combinations of vent geometry, igniter material type and igniter mass, 74 development tests were conducted and reported in References 1 and 2; an additional 15 calibration tests with the baseline igniter have been conducted with BP, $BKNO_3$, NC, MTV, and $BMoO_3$ igniter materials to aid in data reduction

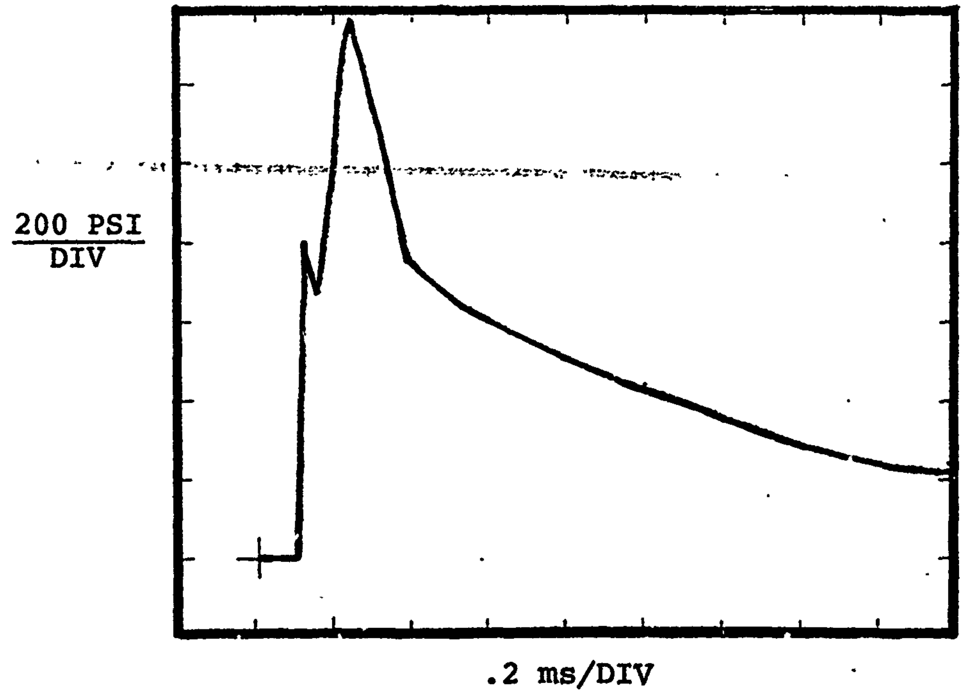

a. Primer Function Test

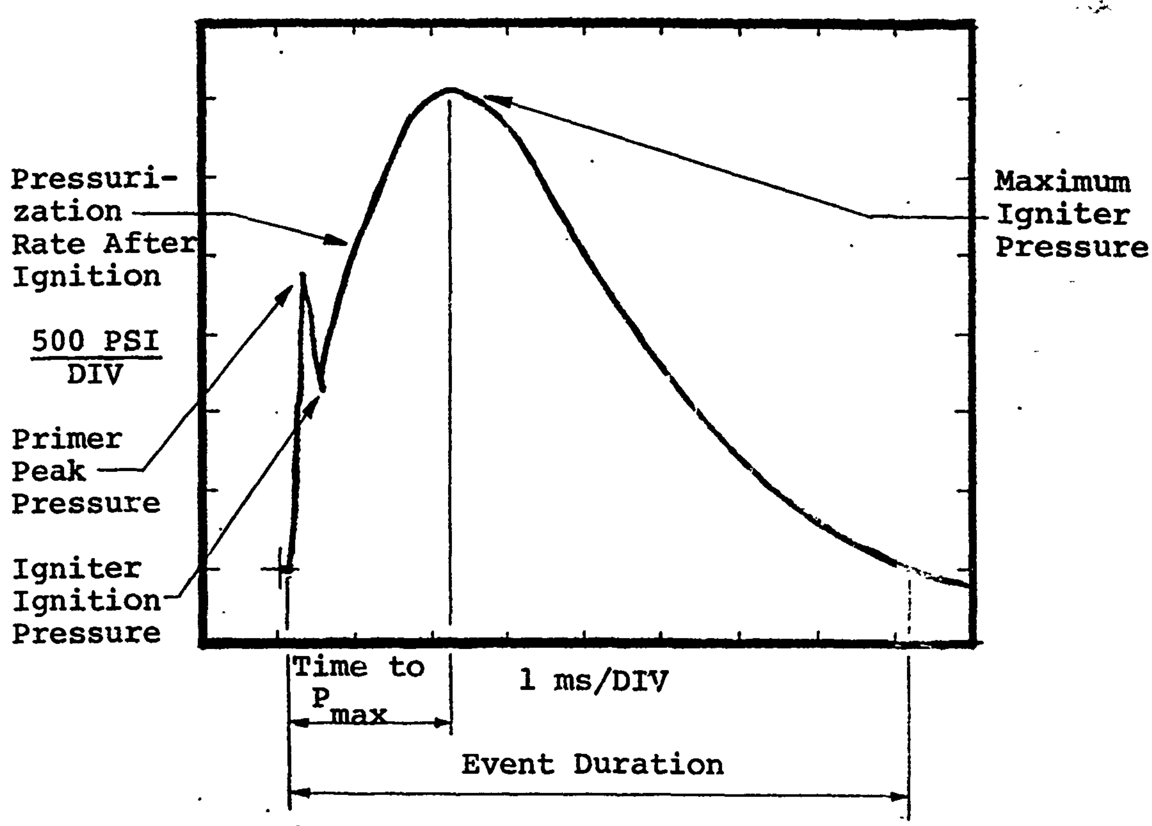

b. Igniter Function Test

Figure 2.3 Pressure-time profiles showing important highlights considered in igniter analysis for the ignition effectiveness tests conducted in the present project.

2.2.2 Ignition Effectiveness Tests

Ignition effectiveness tests were conducted using the IECD with a fixed zone length of inert simulant separating the igniter vent exit and the live propellant zone by 1.5 in (3.8 cm). Ignition effectiveness was determined quantitatively by the amount of thermal energy, based on its heat of explosion, required to ignite the propellant bed 50 percent of the time after filtering through the inert simulant zone. Seventeen (17) experimental series consisting of 287 diagnostic tests were conducted for the following propellant/igniter material combinations:

	Igniter Material				
Propellant	BP	$BKNO_3$	MTV	NC	$BMoO_3$
NACO	x	x	x	x	x
NOSOL-318	x	x	x	x	
NOSOL-363	x	x	x	x	
LOVA	x	x	x	x	

Each experimental series was conducted in order to determine the fifty percent firepoint (energy basis) of the propellant/igniter combination based upon an up-and-down (Bruceton) test technique (Ref. 3). A preliminary series of pre-Brucetons was conducted in order to determine the approximate 50% firepoint as the starting energy level for limited Bruceton series consisting of ten (10) shots each. Test data for each event included a Yes/No fire observation and an in-bore oscilloscope record, Figure 2.4, of the pressure-time profile at the interface of the inert zone and the live propellant zone. A complete run log of the IECD ignition diagnostic tests is included as Appendix A, Tables A-1 through A-4, respectively for:

Table A-1. Series 100: NACO Propellant
Table A-2. Series 200: NOSOL-318 Propellant
Table A-3. Series 300: NOSOL-363 Propellant
Table A-4. Series 400: LOVA Propellant

2.3 Fifty Percent Firepoint Results

Sixteen series of Bruceton tests were conducted to evaluate the ignition effectiveness of BP, $BKNO_3$, NC, and MTV igniter materials with NACO, NOSOL-318, NOSOL-363, and LOVA propellants; one additional series was conducted to evaluate $BMoO_3$ igniter material with NACO propellant. Initial data reduction consisted of reading the oscilloscope records of each shot to record the pertinent pressure-time data indicated in Figure 2.5 and listed below:

1. P_{20} ~ Maximum igniter pressure at entrance to live propellant zone prior to propellant ignition.
2. P_{21} ~ Pressure value at entrance to live propellant zone prior to onset of propellant ignition.
3. P_{2max} ~ Maximum combustion pressure at entrance to live propellant zone during propellant burning.

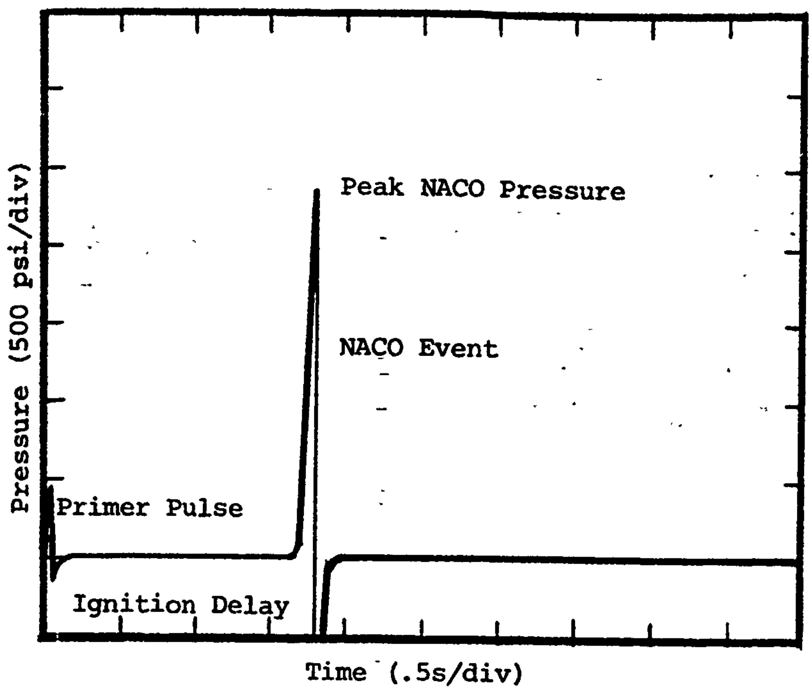

Figure 2.4 IECD Pressure-time Profile Showing Primer Pulse and NACO Combustion

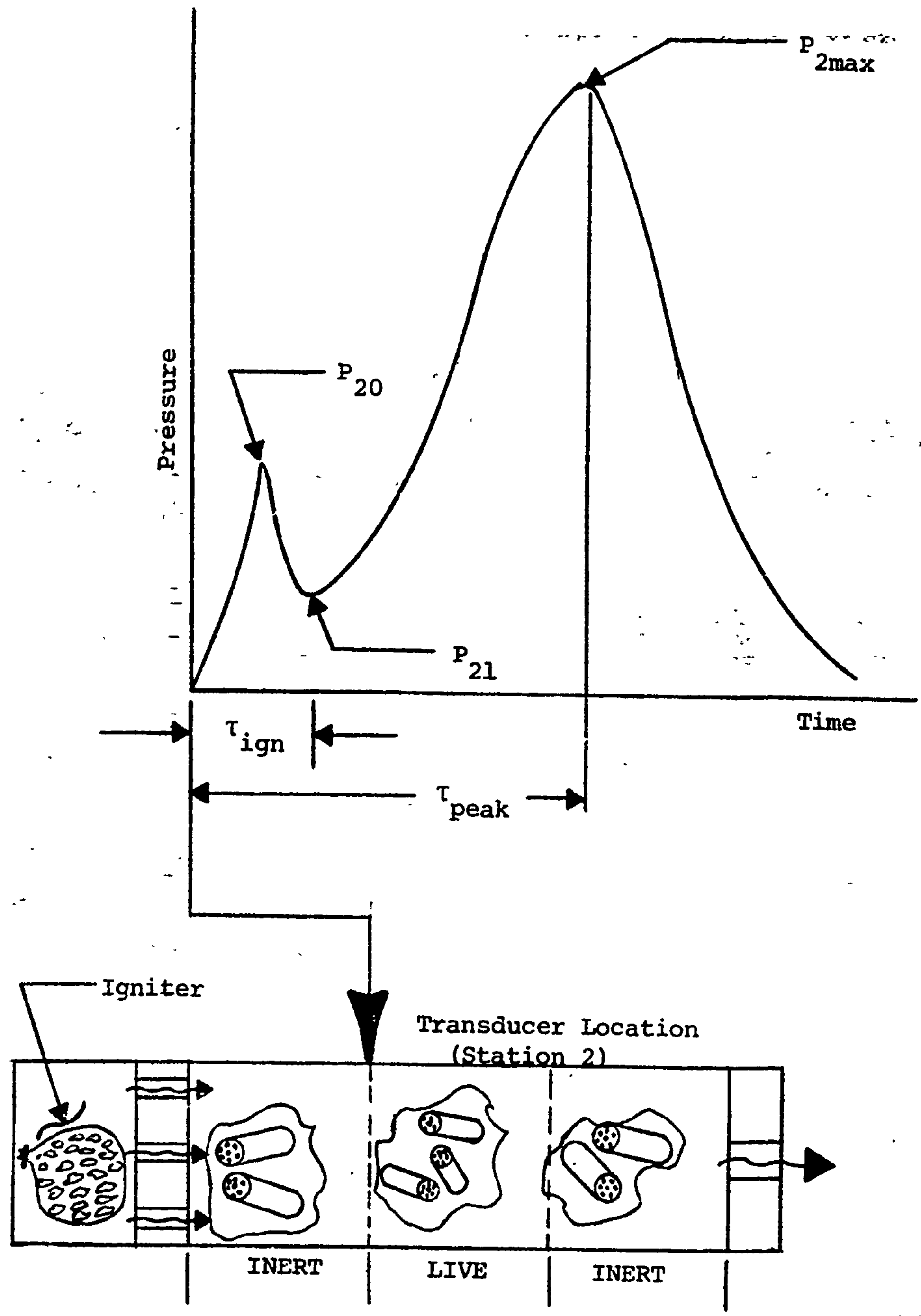

Figure 2.5 Pressure-time Nomenclature Assigned to IECD Data Reduction

4. τ_{ign} ~ Ignition delay time from event initiation to onset of propellant combustion pressure rise.

5. τ_{peak} ~ Time from event initiation to peak propellant combustion pressure.

Data for all seventeen Bruceton ignition effectiveness tests are presented in Appendix B, Tables B-1 through B-20.

The igniter energy flux into the bed was determined for each shot in the test series and plotted against the total igniter energy in Figure 2.6 for NACO, NOSOL-318, and NOSOL-363, respectively. The data for each ignition material are linear with energy flux and separate into two groups, one including BP and $BKNO_3$ and the other containing NC and MTV. Since the test series was conducted with igniter total energy as a control variable for a fixed vent geometry igniter, the energy flux ratio is a result of the test; consequently, it is not currently known if this linear relationship between energy and energy rate is indicative of the igniter housing performance or the igniter material effectiveness. Similar results were observed for LOVA propellant as shown in Figure 2.7. With respect to the LOVA firing data, it should be mentioned that an increased vent size igniter (5115) was utilized to accommodate the larger igniter mass loading required to ignite LOVA propellant.

Each IECD ignition effectiveness test series consisted of 9-12 shots each conducted in an up-down staircase fashion for NACO, NOSOL-318, NOSOL-363, and LOVA propellants. Each test series was statistically reduced using a sensitivity method devleoped by Brownlee and Hodges (Ref. 3) for small samples to determine the

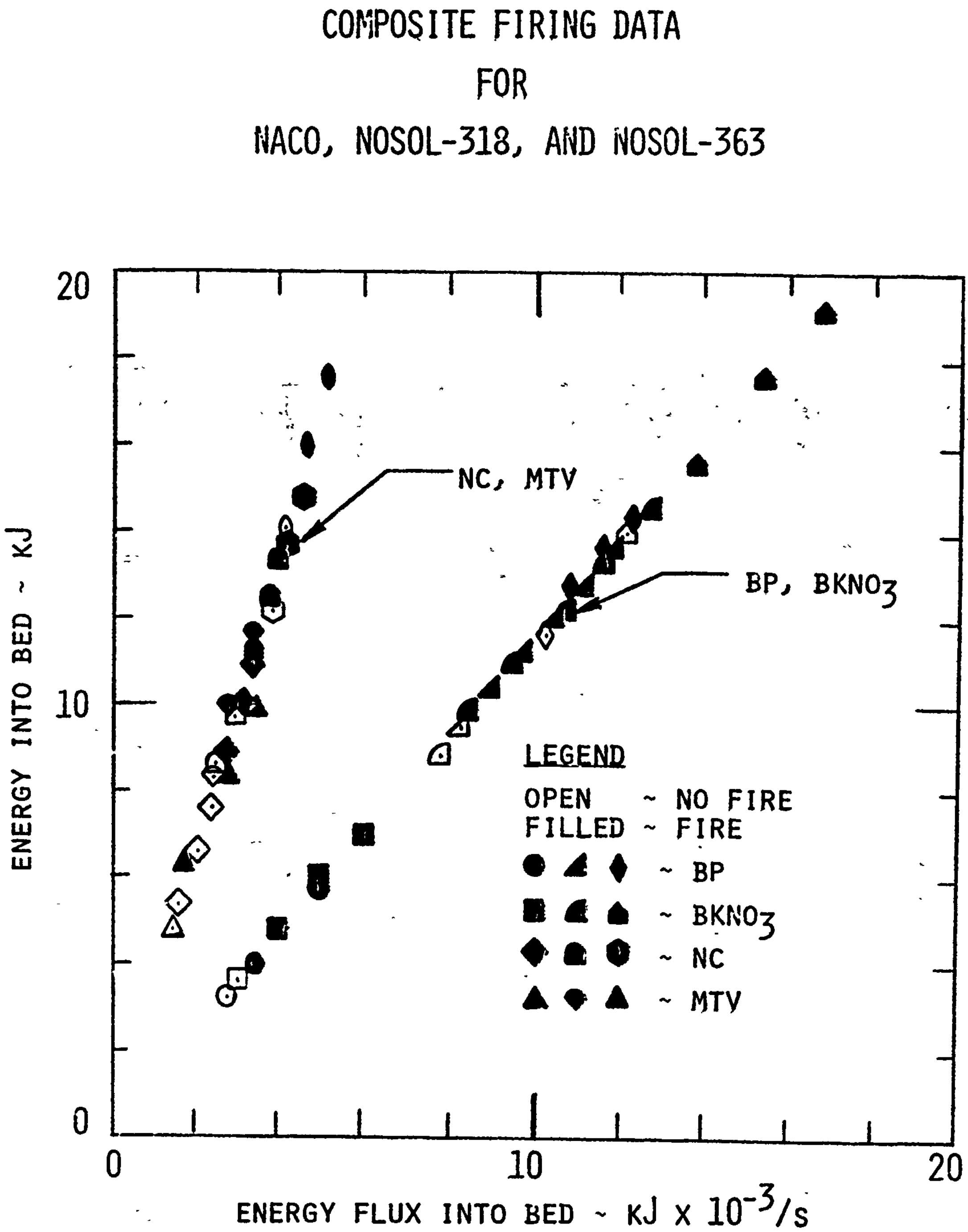

Figure 2.6 Ignition Effectiveness Data for NACO, NOSOL-318 and NOSOL-363

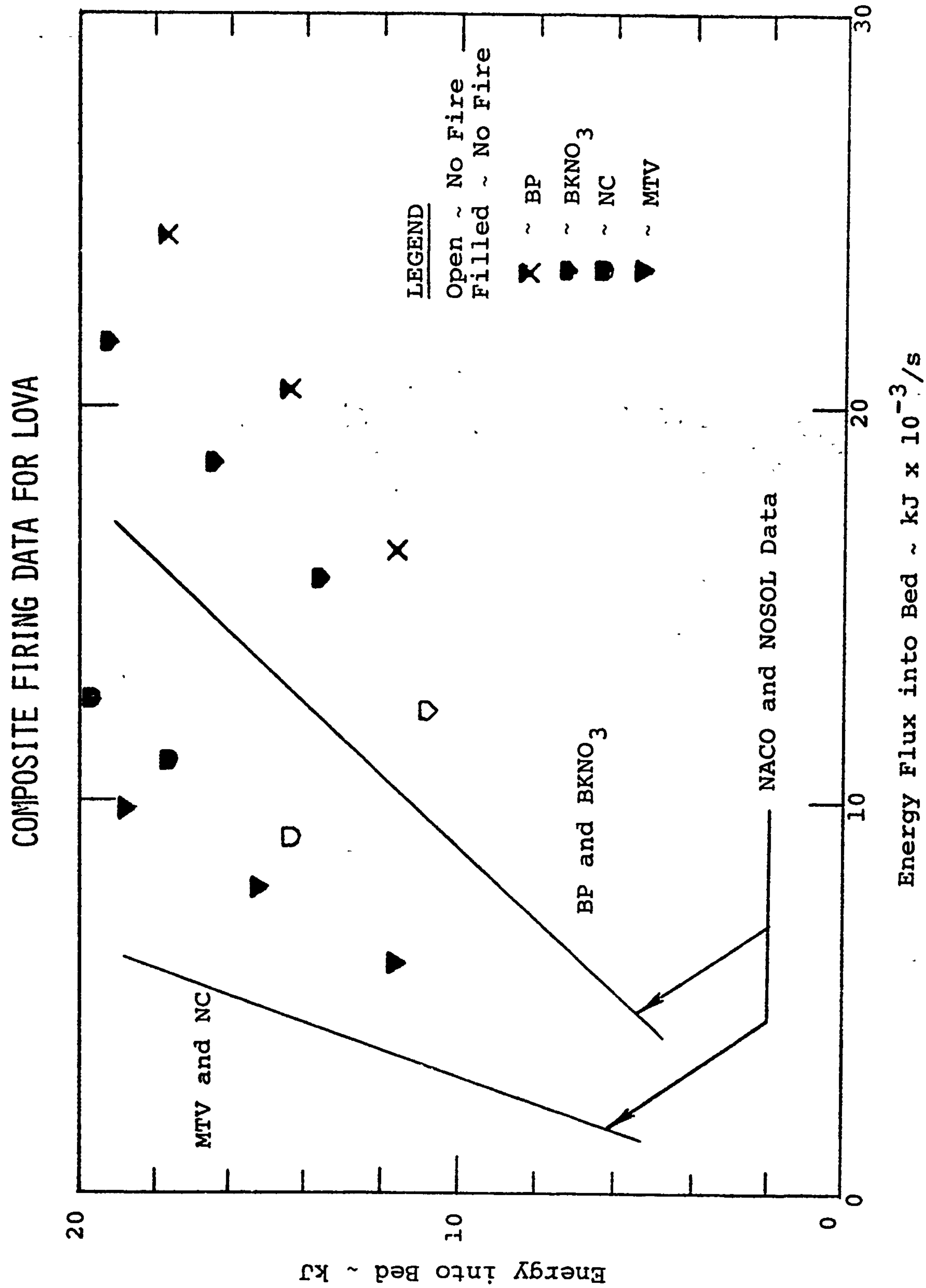

Figure 2.7 Ignition Effectiveness Data for LOVA

50 percent firepoint mean and standard deviation; these Bruceton 50 percent firepoint results are tabulated for each igniter/propellant combination and presented in Appendix C. Based upon the IECD ignition effectiveness data, the following results have been tabulated at the 50 percent mean firepoint for each igniter/propellant combination:

1. Fifty Percent Firepoint Energy Level (Table 2.1)
2. Fifty Percent Firepoint Bed Input Pressure Level (Table 2.2)
3. Fifty Percent Firepoint Relative Ranking Based Upon Energy Level (Table 2.3)

The 50 percent firepoint energy distributions in Table 2.1 indicate that NACO was the easiest propellant to ignite while LOVA was the most difficult, with LOVA requiring approximately 2.5 times as much energy to ignite as NACO. NOSOL-318 was approximately 1.7 times more difficult to ignite than NACO while NOSOL-363 was approximately 2.3 times more difficult to ignite than NACO. For NACO and LOVA propellants, BP and $BKNO_3$ igniter materials were the most effective whereas NC and MTV were the least effective (the $BMoO_3$ results are not included in the present comparisons). For NOSOL-318, MTV, and $BKNO_3$ igniter materials were more effective than BP and NC whereas for NOSOL-363, BP and NC were more effective than MTV and $BKNO_3$.

The IECD data records were reviewed to determine the bed input pressure levels at the 50 percent firepoints. These data, Table 2.2, indicate that, on the average, NACO ignited at bed pressure levels of 165 psia whereas LOVA required higher input pressure levels of 2000 psi. NOSOL-318 ignited at an average

Table 2.1

50% Firepoint Results: Energy Distribution (kJ)

Propellant	Igniter Material BP	$BKNO_3$	NC	MTV	$BMoO_3$
NACO	4.7	5.6	9.6	6.7	12.
N318	12.6	11.3	12.3	9.9	-
N363	13.6	17.9	14.4	16.3	-
LOVA	16.5	16	17.4	17.9	-

Table 2.2

50% Firepoint Results: Bed Input Pressure (psia)

Propellant	Igniter Material BP	$BKNO_3$	NC	MTV	$BMoO_3$
NACO	265	115	120	175	75
N318	1200	425	125	375	-
N363	1350	850	1800	650	-
LOVA	2550	1400	3000	1000	-

Table 2.3

Fifty Percent Firepoint Relative Ranking
Based on Energy Level

Propellant	BP	$BKNO_3$	NC	MTV	$BMoO_3$
NACO	1*	2	4	3	5
N318	4	2	3	1	-
N363	1	4	2	3	-
LOVA	2	1	3	4	-
Total	8	9	12	11	-

* ~ Lowest Energy Level (1)

input pressure of 550 psia whereas NOSOL-363 ignited at approximately 1200 psia. NC igniter material resulted in low pressure ignitions for NACO and NOSOL-318, but required the highest pressure levels for NOSOL-363 and LOVA.

An overall igniter effectiveness ranking based on mean energy levels is presented in Table 2.3 for all igniter materials. Each igniter material is ranked in effectiveness for a given propellant using a score of 1 (lowest energy) to 5 (highest energy) and then totaled for an overall ranking. BP igniter material was most effective for NACO and NOSOL-363, whereas $BKNO_3$ was most effective for LOVA and MTV was most effective for NOSOL-318. Overall effectiveness ranking for the igniter materials for all propellants tested is:

1. BP
2. $BKNO_3$
3. MTV
4. NC

Analyses and implications of these rankings are presented in the next section.

3.0 SUPPORTING ANALYTICAL PROCEDURES

3.1 Qualitative Picture of IECD Ignition Process

The IECD ignition process consists of an igniter jet emerging from a number of axial flow vents and entering a finite thickness bed of inert simulant grains followed by a finite thickness bed of live propellant grains. The igniter jet is comprised of up to four different inert or chemically active stream types:

1. Hot gases
2. Hot vapors capable of undergoing a phase change to either a liquid state or a solid state,
3. Hot liquids capable of undergoing a phase change to a solid state, and
4. Hot solids.

The manner in which the inert simulant bed affects each of these streams is speculation, but is postulated as follows. First, the inert simulant acts as a radiation buffer which is effective in reducing the igniter radiation incident upon the live propellant zone; consequently, the primary propellant ignition stimulus is presumed to be associated with the energy transported by the flowing igniter stream. Under this presumption, it then becomes important to establish the buffering effect of the inert simulant zone upon the multi-phase igniter stream as it flows from the igniter vent through the inert simulant. Since the inert simulant zone consists of a large number of randomly positioned pellets, it is reasonable to assume that the gas stream can pass through the inert bed relatively easily while experiencing a loss in both pressure and temperature prior to entering the live propellant zone, the losses being dependent upon the porosity and length of the inert simulant zone. Considering next the hot vapors, one can presume that the vapors can pass through the inert bed with the same relative ease as the hot gas stream; however, the pressure loss and temperature drop experienced by the gases and vapors would tend to drive the vapors toward a change in phase, presumably to a liquid which would be relatively effective in the inert heating phase of the live propellant ignition process. With regard to the hot liquids contained in the igniter stream, one can envision that the inert zone pellets may become wetted by the liquid stream during the flow process, thus reducing the initial liquid content potentially available for the live propellant zone. Of perhaps more significance is the possibility that the liquids initially present in the igniter products may undergo a phase change from liquid to solid within the confines of the inert zone, thus significantly reducing the potential effectiveness of the igniter stream to initiate combustion in the live propellant zone. Finally, if one applies the previous logic to the igniter solids flowing through the inert simulant bed, the higher trajectory momentum of the solids makes them less capable of traversing the inert zone without impacting the inert simulant pellets and becoming trapped in the inert zone, thus reducing the ignition potential of the igniter stream.

3.2 Igniter Simulation

Following the work of Kuo (Ref. 4), the IECD igniter system is treated as a quasi-steady, one-dimensional flow of an ideal gas. Referring to the igniter control volume shown schematically in Figure 3.1, igniter gases are generated from the burning

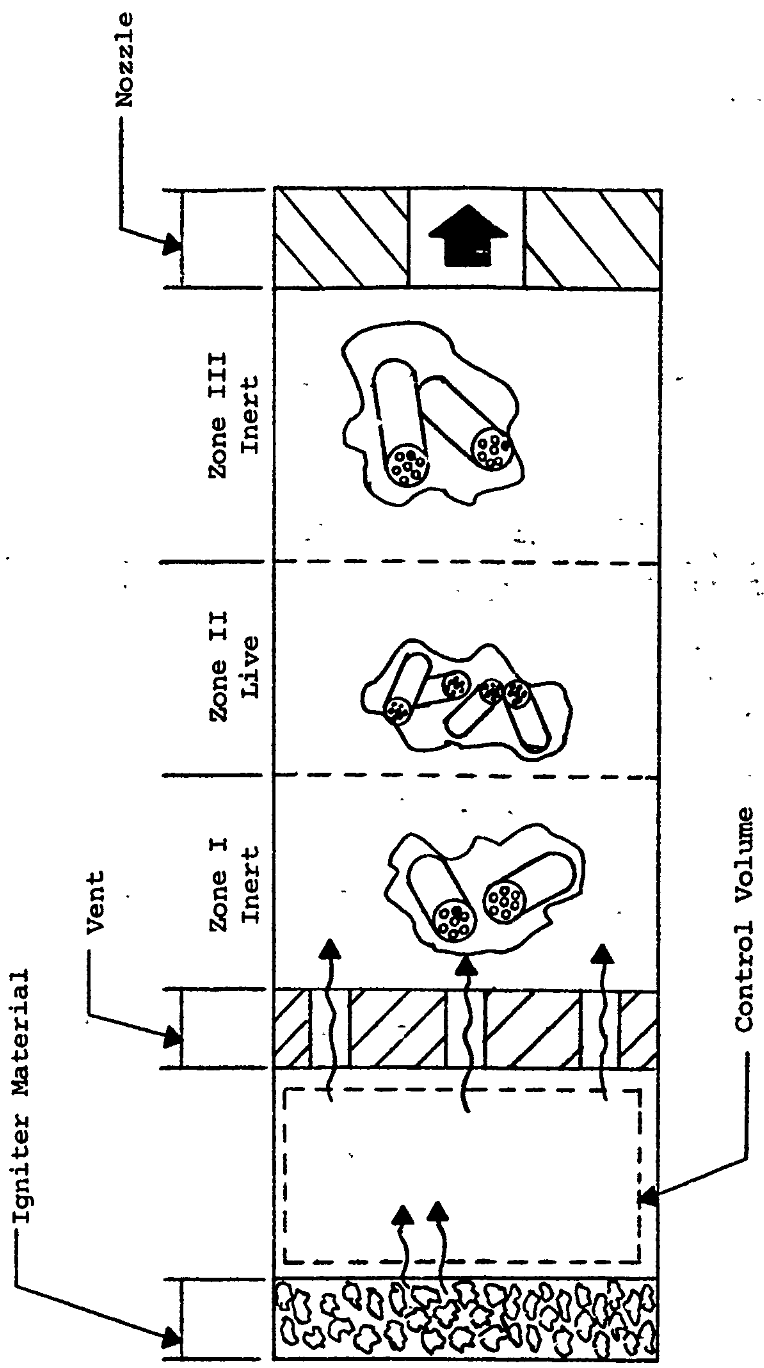

Figure 3.1 Schematic Representation of IECD Showing Igniter Control Volume

solid and introduced into the igniter control volume at a rate $\dot{m}_s$ equal to the igniter mass generation rate. Conservation of mass coupled with the ideal gas law gives

$$\frac{P_c}{RT_c}\frac{\dot{m}_s}{\rho_s} + V_c \frac{d}{dt}\left(\frac{P_c}{RT_c}\right) = \dot{m}_s - \dot{m}_{out} \qquad (1)$$

where

P_c = igniter chamber pressure
T_c = igniter chamber temperature
V_c = igniter chamber free volume
ρ_s = density of igniter material

The igniter exit flow, $\dot{m}_{out}$, may consist of gases, vapors, liquids and solids, all flowing with the mean gas velocity as calculated from one-dimensional, ideal flow theory. Equation (1) may be solved for the rate of temperature change in the control volume to give

$$\frac{dT_c}{dt} = \frac{T_c}{P_c}\frac{dP_c}{dt} + \frac{RT_c{}^2}{V_c P_c}\dot{m}_s\left(\frac{P_c}{RT_c\rho_s} - 1\right) + \frac{RT_c{}^2}{V_c P_c}\dot{m}_{out} \qquad (2)$$

Conservation of energy applied to the igniter gas phase gives

$$\frac{d}{dt}\left(\frac{P_c C_v V_c}{R}\right) = \dot{m}_s C_p T_f - \dot{m}_{out}(C_p T_{out} + \tfrac{1}{2}V_{out}{}^2) \qquad (3)$$

where it has been assumed that the gases entering the control volume from the burning surface are at the adiabatic flame temperature, T_f. Equation (3) can be solved for the igniter mass generation rate, $\dot{m}_s$, in terms of igniter variables and the exit mass flow rate, $\dot{m}_{out}$, according to

$$\dot{m}_s = \frac{V_c \frac{dP_c}{dt} + (\gamma-1)\dot{m}_{out}(C_pT_c)_{out}}{(\gamma-1)C_pT_f - \frac{P_c}{\rho_s}} \quad (4)$$

If the exit flow is assumed to consist of gases and vapors which behave as gases and liquids and solids which travel as a condensed phase with the gas flow field, then

$$\dot{m}_{out} = \dot{m}_g + \dot{m}_{cp} \quad (5)$$

In the present simplified treatment of the igniter system, not enough information is available to adequately predict the condensed phase exit flow rate, so the assumption is made that the condensed flow rate is proportional to the igniter mass generation rate, $\dot{m}_s$

$$\dot{m}_{cp} = \beta\dot{m}_s \quad (6)$$

Substituting equations (5) and (6) into equation (4) gives a relationship for $\dot{m}_s$ in terms of the experimentally measured igniter pressure, P_c,

$$\dot{m}_s = \frac{V_c \frac{dP_c}{dt} + (\gamma-1)C_pT_c\dot{m}_g}{(\gamma-1)C_pT_f - (\gamma-1)C_pT_c - \frac{P_c}{\rho_s}} \quad (7)$$

For ideal, one-dimensional flow, the exit gas flow rate, $\dot{m}_g$, is given by

$$\dot{m}_g = \frac{P_cA_e}{\sqrt{RT_c}} \quad (8)$$

where A_e = vent exit area.

Equations (2), (7), and (8) characterize the igniter behavior in terms of thermochemical data, igniter geometry, experimentally measured pressure data, and the unknown condensed phase fraction, β. Using the assumption that igniter burnout occurs at igniter peak pressure, the cast of equations may be iteratively solved using assumed values of β subject to the constraint that the integral of the igniter mass generation rate over the burning period is equal to the amount of igniter mass used to conduct the experiment.

The equations have been formulated into a computer model and solved for each of the igniter materials used in the current project, as illustrated in Figures 3.2 through 3.4. The igniter calibration pressure-time profile is shown in Figure 3.2 for 2 g of black powder for the baseline vent configuration (4080AV) and is used as the "input" curve for P_c and dP_c/dt in the analytical model. Mass flow rates for the gas-vapor phase and the condensed phases are shown in Figure 3.3 and indicate that, at peak conditions, the condensed phase to gas phase mass flow ratio is about 0.20. Using the mass flow rates presented in Figure 3.3, the igniter energy flux into the bed is calculated for the gas phase, $\dot{E}_g$, and the condensed phase, $\dot{E}_{cp}$, respectively, by

$$\dot{E}_g = \dot{m}_g \left[\frac{2C_p T_c}{(\gamma+1)} + \frac{\gamma}{(\gamma+1)} RT_c \right] \tag{9}$$

and

$$\dot{E}_{cp} = \dot{m}_{cp} \left[C_{p_{cp}} T_f + \frac{\gamma}{\gamma+1} RT_c \right] \tag{10}$$

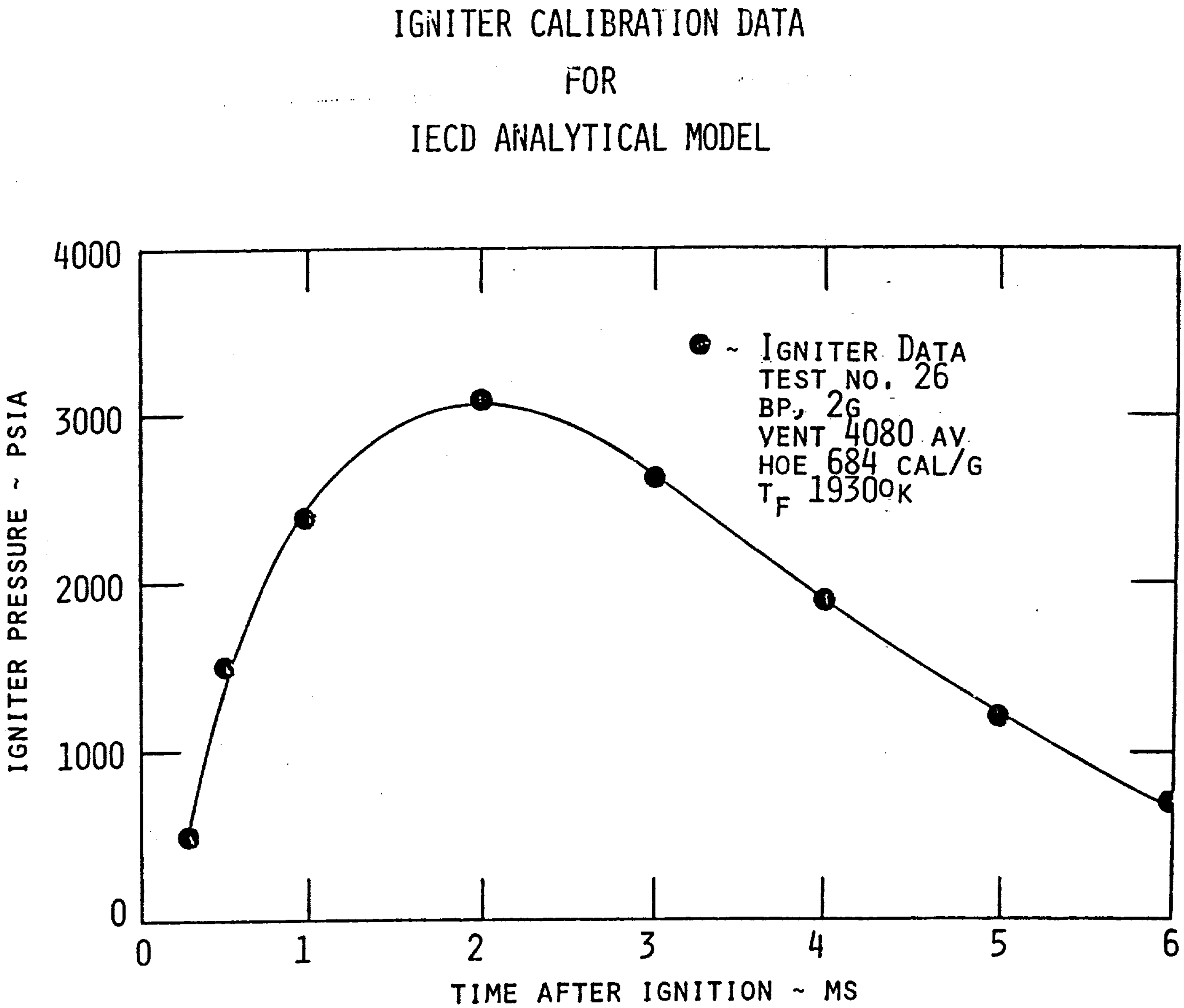

Figure 3.2 Igniter Calibration Data for IECD Analytical Model

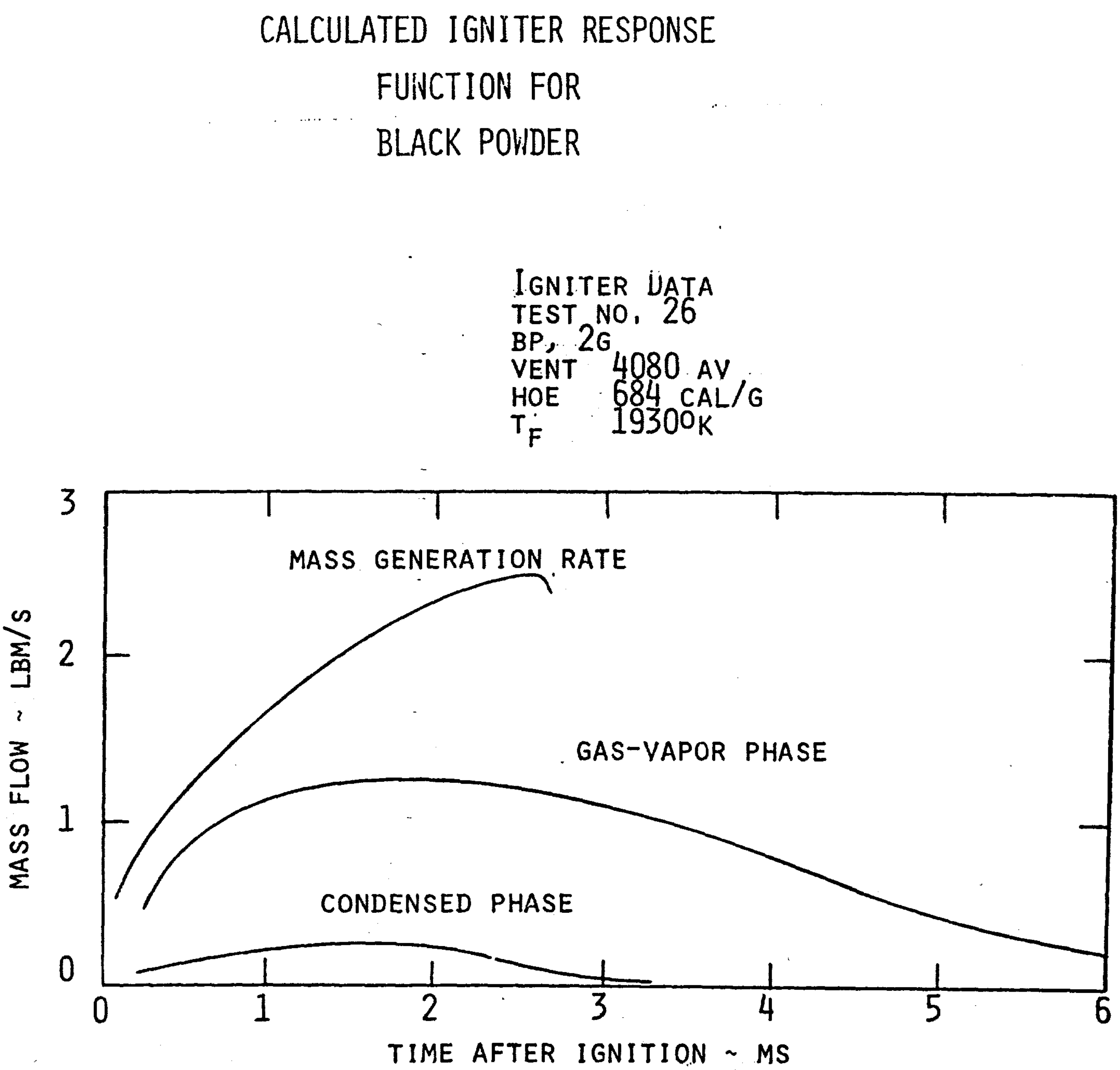

Figure 3.3 Calculated Igniter Response Function for Black Powder

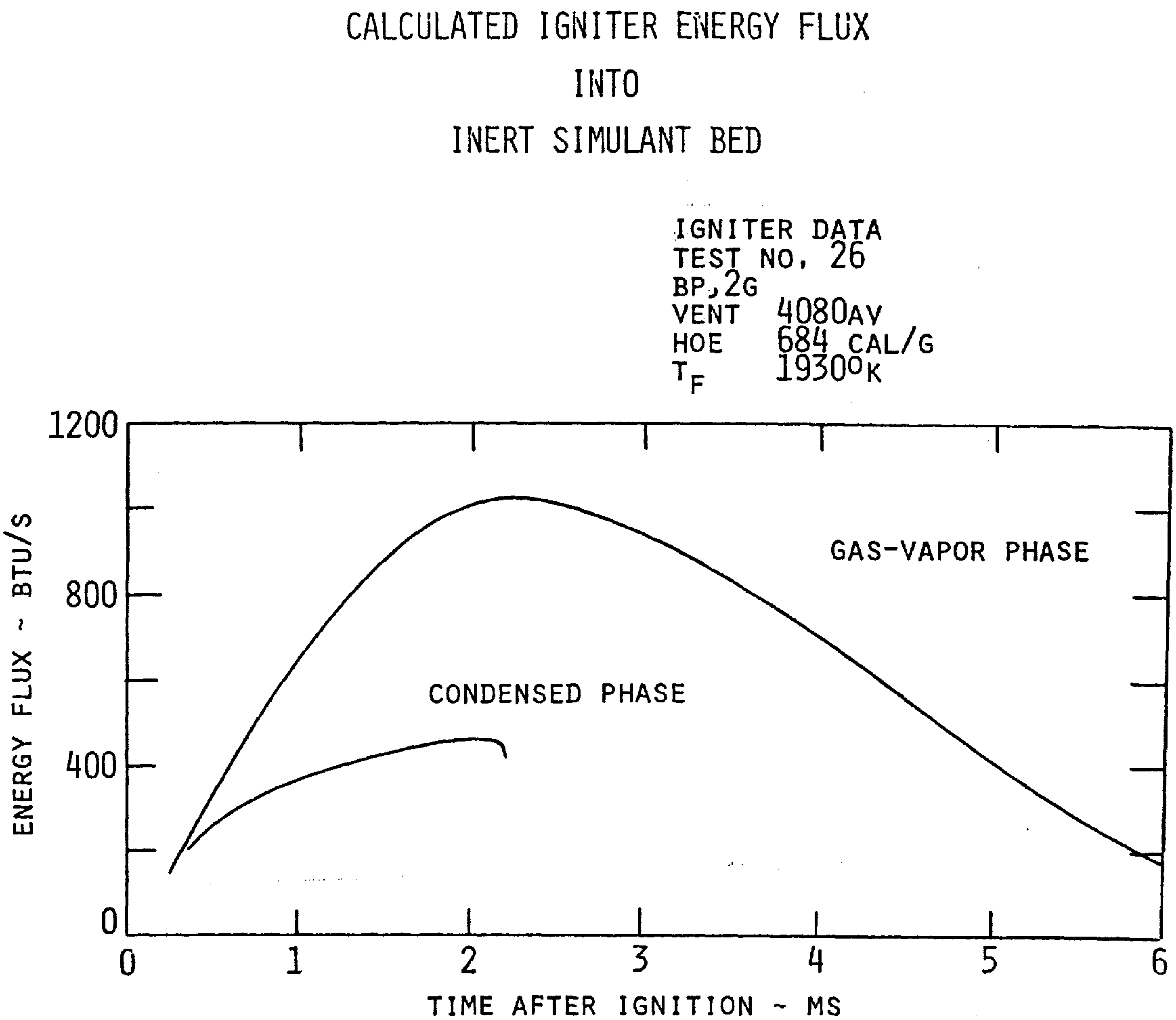

Figure 3.4 Calculated Igniter Energy Flux into Inert Simulant Bed

where the condensed phase liquids and solids are assumed to be generated at the adiabatic flame temperature and are not permitted to equilibrate with the gas temperature, T_c. Energy flux rates for the case in consideration are presented in Figure 3.4 and indicate that, at peak conditions, the condensed phase to gas phase energy flux ratio is about 0.45.

Igniter calibration data have been combined with the analytical model to generate a set of working curves to facilitate data reduction of the IECD ignition effectiveness test results; these results are presented in Appendix D.

3.3 Igniter Effectiveness Rankings

Based upon the previous qualitative picture of the IECD ignition process, an expression for the dependence of convective heat transfer to the bed was developed with respect to the thermodynamic and transport properties of the igniter product stream. An expression for the inert gas phase is offered and used as a basis for applying augmentation factors for the increased density vapor, liquid, and solid phases. The base expression and the augmentation factors were evaluated using thermochemical code values and used as the basis for ranking the effectiveness of the different ignition stimuli.

The convective heat transfer from the hot igniter stream may be functionally expressed as

$$\frac{\dot{Q}}{A} \sim h_e^*(T_p - T_g) \qquad (11)$$

where h_e = Effective heat transfer coefficient for composite stream

T_p = Inert simulant, or propellant temperature

T_g = Temperature of igniter gas stream.

The heat transfer coefficient is generally proportional to the specific heat, the density, and the velocity of the flowing stream, or

$$h \sim C_p \rho V \tag{12}$$

If the effective heat transfer coefficient for the composite igniter stream is based upon the gas phase, then it will be assumed that the effective heat transfer coefficient is given by

$$h_e \sim h_g (1 + I)(1 + J)(1 + K) \tag{13}$$

where I, J, and K are the vapor, liquid, and solid phase augmentation factors and h_g is the gas phase heat transfer coefficient.

Since I, J, and K are proportional to the mass flux per unit area of the composite flow field, it seems reasonable to represent I, J, and K by the product fraction mass ratios, as determined by thermochemical code calculations, multiplied by the ratio of specific heats of the phase in question divided by the gas phase specific heat, or

$$I = \frac{C_{pv}}{C_p} * (\text{Vapor mass fraction})$$

$$J = \frac{C_{pl}}{C_p} * (\text{Liquid mass fraction}) \tag{14}$$

$$K = \frac{C_s}{C_p} * (\text{Solid mass fraction})$$

Igniter material characterizations based upon NASA Lewis code results at a chamber pressure of 500 psi, Table 3.1, have been used to determine augmentation factors for BP, $BKNO_3$, NC, MTV, and $BMoO_3$ as shown in Table 3.2.

Table 3.1

INERT GAS PHASE HEATING AUGMENTATION FACTORS

Item	BP	BKN	NC	MTV	$BMoO_3$
			IGNITER MATERIAL		
Gas phase mass fraction	.548	.247	.902	.003	.127
Vapor phase mass fraction	.01	.549	0	.396	.018
Liquid phase mass fraction	.409	.035	.006	.477	.302
Solid phase mass fraction	.024	.169	0	.124	.558
C_{pV}/C_p (Assumed)	1.1	1.1	1.1	1.1	1.1
C_{pl}/C_p (Assumed)	1.7	1.7	1.7	1.7	1.7
C_s/C_p (Assumed)	1.3	1.3	1.3	1.3	1.3
I (Vapor)	.01	.61	0	.44	.02
J (Liquid)	.70	.06	0	.81	.51
K (Solid)	.03	.22	0	.16	.73

Table 3.2

IGNITER MATERIAL CHARACTERIZATION

Item	BP	$BKNO_3$	NC	MTV	$BMoO_3$
	IGNITER MATERIAL				
Density (g/cc)	1.6	1.4	1.2	1.5	1.7
HOE (cal/g)	684	1500	965	1450	500
Flame Temperature (T_p, °K)	1930	2895	2350	2650	2390
Gas Constant ($ft\text{-}lb_f/lbm\text{-}°R$)	28	25	62	26	27
Specific Heat, C_p (BTU/lbm-°R)	.62	1.61	.46	1.01	1.41
Ratio of Specific Heats	1.11	1.08	1.22	1.09	1.04
Molecular Weight	56	63	25	60	58
Production Fraction (% Weight)					
Vapor-Solid	1.0	54.9	0	39.6	1.8
Liquid-Solid	40.9	3.5	0.6	47.7	30.2
Solid	0	16.9	0	12.4	55.8
Total Solid @14.7 psi	41.9	75.3	0.6	99.7	87.8
Gas	54.8	24.7	90.2	0.3	12.2
Total	96.7*	100.0	90.8*	100.0	100.0

*Balance Water Vapor

In order to calculate a relative number for the gas phase heat transfer coefficient, the following argument based upon transport theory is given:

$$h_g \sim C_p \rho V \quad (15)$$

$$\sim C_p M R^{1/2} T^{1/2}$$

$$\sim C_p M^{1/2} T^{1/2}$$

The overall heat transfer to the bed is then proportional to

$$\left.\frac{\dot{Q}}{A}\right]_g \sim C_p M^{1/2} T^{3/2} \quad (16)$$

Equation (16) will be used as the inert heat transfer base for the gas phase and modified by the augmentation factors to indicate the overall effectiveness of the igniter materials according to

$$\left.\frac{\dot{Q}}{A}\right]_{eff} \sim C_p M^{1/2} T^{3/2} (1+I)(1+J)(1+K) \quad (17)$$

Calculated performance factors for the igniter materials tested in the current project are presented in Table 3.3 and relative rankings are presented in Table 3.4. These results suggest that the effective stimuli for each igniter material is as follows:

Overall Calculated Ranking	Material	Effective Stimuli
1 (Best)	MTV	Liquids, vapors
2	$BKNO_3$	Gases, vapors, and solids
3	BP	Liquids
4 (Worst)	NC	Gases

Table 3.3

Calculated Performance Factors of Igniter Materials

Item	BP	$BKNO_3$	NC	MTV	$BMoO_3$
Hot Gas ($C_pM^{1/2}T^{1/2}$)	1.01	1.23	1.11	1.18	1.12
Vapor (1+I)	1.01	1.6	1.0	1.4	1.02
Liquid (1+J)	1.7	1.06	1.0	1.8	1.5
Solid (1+K)	1.03	1.2	1.0	1.16	1.7
Effective Composite	1.8	2.5	1.1	3.4	2.9

Table 3.4

Calculated Relative Ranking of Igniter Materials

		Igniter Characteristic Stimuli			
Ranking	Overall	Gases	Vapors	Liquids	Solids
1 (Best)	MTV	$BKNO_3$	$BKNO_3$	MTV	$BKNO_3$
2	$BKNO_3$	MTV	MTV	BP	MTV
3	BP	NC	BP	$BKNO_3$	BP
4 (Worst)	NC	BP	NC	NC	NC

The calculated rankings and the experimentally determined rankings based upon 50 percent firepoint energy levels are given below:

Overall Ranking	Calculated Ranking	50% Firepoint Ranking
1 (Best)	MTV	BP
2	$BKNO_3$	$BKNO_3$
3	BP	MTV
4	NC	NC

The experimentally determined number one ranking for BP suggests that the BP product liquids are very effective in penetrating the inert simulant bed without undergoing a phase change to the solid state, whereas the liquid phase in the MTV product steam is not. This ranking observation between BP and MTV is consistent with the experimental observation that round, frozen molten spheres of metal were found in the MTV firings indicating that this effective heating stimuli was filtered out by the inert simulant bed.

The $BKNO_3$ effective stimuli appears to be the high concentration of vapors in the reaction products. Since the combined fraction of vapors, liquids, and solids is higher for $BKNO_3$ than BP, it appears that the inert simulant bed was effective in preventing all, or part, of the solid phase energy from reaching the live propellant zone.

The experimentally observed rankings for MTV and NC firings were a close 3 and 4, respectively. The last place results of NC suggest that a high gas output igniter system in the absence of vapors, solids, and liquids, is not very effective. As mentioned earlier, it appears that a large portion of the MTV liquids experienced a phase change, thus suggesting that the effective MTV ignition stimuli is via the vapor phase.

4.0 REFERENCES

1. Martino, J., Hassler, T., and Varney, M., "An Exploratory Investigation of the Influence of Igniter Chemistry on Ignition in Porous Bed Gun Propellants: Phase I. Igniter Development," Final Technical Report on Contract N00174-80-C-0138, ACT-TR-8125, April 1981.

2. Martino, J. and Varney, M., "An Exploratory Investigation of the Influence of Igniter Chemistry on Ignition in Porous Bed Gun Propellants: IECD Combustion Tests," Final Technical Report on Contract N00174-80-C 0138 Mod P00002, ACT-TR-8125-2, September 1981.

3. Brownlee, K. A., Hodges, J. L., and Rosenblatt, M., "The Up-and-Down Method with Small Samples," J. of American Statistical Association, Volume 48, 1953.

4. Kuo, K. K., Moore, B. B., and Chen, D. Y., "Characterization of Mass Flow Rates for Various Percussion Primers," Seventh International Colloquim on Gasdynamics of Explosions and Reactive Systems, Gottingen, West Germany, August 1979.

APPENDIX A

IECD EXPANDED IGNITION DIAGNOSTIC TESTS

Table A-1	Series 100:	NACO
Table A-2	Series 200:	NOSOL-318 Propellant
Table A-3	Series 300:	NOSOL-363 Propellant
Table A-4	Series 400:	LOVA Propellant

TABLE A-1

IECD EXPANDED IGNITION DIAGNOSTIC TESTS

(Inert Simulant Zone 1 Thickness 1.50 in)

Series 100: NACO Propellant

Test Number	Igniter Configuration	Material	Mass (g)	δm (g)	Propellant Material	Propellant Mass (g)	Ignition (Yes/No)
101E	4080AV-R	BP	.6	.1	NACO	40	N
102E	4080AV-R	BP	.7	.1	NACO	40	N
103E	4080AV-R	BP	.8	.1	NACO	40	N
104E	4080AV-R	BP	.9	.1	NACO	40	N
105E	4080AV-R	BP	1.0	.1	NACO	40	N
106E	4080AV-R	BP	1.31	.1	NACO	40	N
107E	4080AV	BP	1.31	.1	NACO	40	Y
108E	4080AV	BP	1.0	.1	NACO	40	Y
101	4080AV	BP	.7	.1	NACO	40	N
102	4080AV	BP	.8	.1	NACO	40	N
103	4080AV	BP	.9	.1	NACO	40	Y
104	4080AV	BP	.8	.1	NACO	40	N
105	4080AV	BP	.9	.1	NACO	40	N
106	4080AV	BP	1.0	.1	NACO	40	N
107	4080AV	BP	1.1	.1	NACO	40	Y
108	4080AV	BP	1.0	.1	NACO	40	N
109	4080AV	BP	1.1	.1	NACO	40	N
110	4080AV	BP	1.2	.1	NACO	40	N
111	4080AV	BP	1.3	.1	NACO	40	N
112	4080AV	BP	1.4	.1	NACO	40	N
113	4080AV	BP	1.5	.1	NACO	40	N
114	4080AV	BP	1.6	.1	NACO	40	N
115	4080AV	BP	1.2	.3	NACO	40	N
116	4080AV	BP	1.5	.3	NACO	40	N
117	4080AV	BP	1.8	.3	NACO	40	N
118	4080AV	BP	2.1	.3	NACO	40	Y

Test Number	Igniter Configuration	Material	Mass (g)	δm (g)	Propellant Material	Propellant Mass (g)	Ignition (Yes/No)
119	4080AV	BP	1.8	.3	NACO	40	Y
120	4080AV	BP	1.5	.3	NACO	40	N
121	4080AV	BP	1.8	.3	NACO	40	Y
122	4080AV	BP	1.5	.3	NACO	40	Y
123	4080AV	BP	1.2	.3	NACO	40	N
124	4080AV	BKN	.8	.2	NACO	40	Y
125	4080AV	BKN	.6	.2	NACO	40	N
126	4080AV	BKN	.8	.2	NACO	40	N
127	4080AV	BKN	1.0	.2	NACO	40	N
128	4080AV	BKN	1.2	.2	NACO	40	Y
129	4080AV	BKN	1.0	.2	NACO	40	Y
130	4080AV	BKN	.8	.2	NACO	40	N
131	4080AV	BKN	1.0	.2	NACO	40	Y
132	4080AV	BKN	.8	.2	NACO	40	Y
133	4080AV	NC	1.4	.3	NACO	40	N
134	4080AV	NC	1.7	.3	NACO	40	N
135	4080AV	NC	2.0	.3	NACO	40	N
136	4080AV	NC	2.3	.3	NACO	40	N
137	4080AV	NC	2.6	.3	NACO	40	Y
138	4080AV	NC	2.3	.3	NACO	40	Y
139	4080AV	NC	2.0	.3	NACO	40	N
140	4080AV	NC	2.3	.3	NACO	40	Y
141	4080AV	NC	2.0	.3	NACO	40	N
142	4080AV	NC	2.3	.3	NACO	40	N
143	4080AV	NC	2.6	.3	NACO	40	N
144	4080AV	NC	2.9	.3	NACO	40	Y
145	4080AV	MTV	1.2	.3	NACO	40	N
146	4080AV	MTV	2.0	.3	NACO	40	Y
147	4080AV	MTV	1.7	.3	NACO	40	Y
148	4080AV	MTV	1.4	.3	NACO	40	Y

Test Number	Igniter Configuration	Material	Mass (g)	δm (g)	Propellant Material	Propellant Mass (g)	Ignition (Yes/No)
149	4080AV	MTV	1.1	.3	NACO	40	N
150	4080AV	MTV	1.4	.3	NACO	40	Y
151	4080AV	MTV	1.1	.3	NACO	40	N
152	4080AV	MTV	1.4	.3	NACO	40	Y
153	4080AV	MTV	1.1	.3	NACO	40	Y
154	4080AV	MTV	.8	.3	NACO	40	N
155	4080AV	MTV	1.1	.3	NACO	40	Y
156	4080AV	MTV	.8	.3	NACO	40	N
157	4080AV	BMO	3.0	.5	NACO	40	N
158	4080AV	BMO	5.0	.5	NACO	40	Y
159	4080AV	BMO	4.0	.5	NACO	40	N
160	4080AV	BMO	4.5	.5	NACO	40	N
161	4080AV	BMO	5.0	.5	NACO	40	N
162	4080AV	BMO	5.5	.5	NACO	40	N
163	4080AV	BMO	6.0	.5	NACO	40	Y
164	4080AV	BMO	5.5	.5	NACO	40	Y
165	4080AV	BMO	5.0	.5	NACO	40	N
166	4080AV	BMO	5.5	.5	NACO	40	Y
167	4080AV	BMO	5.0	.5	NACO	40	N
168	4080AV	BMO	5.5	.5	NACO	40	N
169	4080AV	BMO	6.0	.5	NACO	40	N
170	4080AV	BMO	6.5	.5	NACO	40	Y
171	4080AV	BMO	6.0	.5	NACO	40	N
172	4080AV	BMO	6.5	.5	NACO	40	N

TABLE A-2

IECD EXPANDED IGNITION DIAGNOSTIC TESTS

(Inert Simulant Zone 1 Thcikness 1.50 in)

Series 200: NOSOL-318 Propellant

Test Number	Igniter Configuration	Material	Mass (g)	δm (g)	Propellant Material	Propellant Mass (g)	Ignition (Yes/No)
201	4080AV	BP	1.65	.6	N318	40	N
202	4080AV	BP	2.25	.6	N318	40	Y
203	4080AV	BP	1.65	.6	N318	40	N
204	4080AV	BP	2.25	.6	N318	40	N
205	4080AV	BP	2.85	.6	N318	40	N
206	4080AV	BP	3.45	.6	N318	40	N
207	4080AV	BP	4.05	.6	N318	40	N
208	4080AV	BP	3.45	.6	N318	40	Y
209	4080AV	BP	2.00	.6	N318	40	N
210	4080AV	BP	3.00	.6	N318	40	Y
211	4080AV	BP	4.65	.6	N318	40	N
212	4080AV	BP	5.25	.6	N318	40	Y
213	4080AV	BP	4.65	.6	N318	40	N
214	4080AV	BP	5.25	.6	N318	40	Y
215	4080AV	BP	4.65	.6	N318	40	Y
216	4080AV	BP	4.05	.6	N318	40	N
217			No Test Conducted				
218	4080AV	BP	4.70	.3	N318	40	N
219	4080AV	BP	5.00	.3	N318	40	Y
220	4080AV	BP	4.70	.3	N318	40	Y
221	4080AV	BP	4.40	.3	N318	40	N
222	4080AV	BP	4.70	.3	N318	40	Y
223	4080AV	BP	4.40	.3	N318	40	N
224	4080AV	BP	4.70	.3	N318	40	Y
225	4080AV	BP	4.40	.3	N318	40	Y
226	4080AV	BP	4.10	.3	N318	40	Y

Test Number	Igniter Configuration	Material	Mass (g)	δm (g)	Propellant Material	Propellant Mass (g)	Ignition (Yes/No)
227	4080AV	BP	3.80	.3	N318	40	Y
228	4080AV	BP	3.50	.3	N318	40	N
229	4080AV	BP	3.80	.3	N318	40	Y
230	4080AV	BKN	2.00	.5	N318	40	N
231	4080AV	BKN	2.50	.5	N318	40	Y
232	4080AV	BKN	2.00	.5	N318	40	N
233	4080AV	BKN	2.50	.2	N318	40	Y
234	4080AV	BKN	2.30	.2	N318	40	Y
235	4080AV	BKN	2.10	.2	N318	40	Y
236	4080AV	BKN	1.90	.2	N318	40	N
237	4080AV	BKN	2.10	.2	N318	40	Y
238	4080AV	BKN	1.90	.2	N318	40	Y
239	4080AV	BKN	1.70	.2	N318	40	N
240	4080AV	BKN	1.90	.2	N318	40	Y
241	4080AV	BKN	1.70	.2	N318	40	N
242	4080AV	BKN	1.90	.2	N318	40	Y
243	4080AV	BKN	1.70	.2	N318	40	Y
244	4080AV	BKN	1.50	.2	N318	40	N
245	4080AV	BKN	1.70	.2	N318	40	Y
246	4080AV	NC	5.00	1.0	N318	40	Y
247	4080AV	NC	4.00	1.0	N318	40	Y
248	4080AV	NC	3.00	1.0	N318	40	Y
249	4080AV	NC	2.00	1.0	N318	40	N
250	4080AV	NC	2.30	.3	N318	40	N
251	4080AV	NC	2.60	.3	N318	40	N
252	4080AV	NC	2.90	.3	N318	40	N
253	4080AV	NC	3.20	.3	N318	40	Y
254	4080AV	NC	2.90	.3	N318	40	N
255	4080AV	NC	3.20	.3	N318	40	Y
256	4080AV	NC	2.90	.3	N318	40	N

Test Number	Igniter Configuration	Material	Mass (g)	δm (g)	Propellant Material	Propellant Mass (g)	Ignition (Yes/No)
257	4080AV	NC	3.20	.3	N318	40	N
258	4080AV	NC	3.50	.3	N318	40	Y
259	4080AV	NC	3.20	.3	N318	40	Y
260	4080AV	NC	2.90	.3	N318	40	Y
261	4080AV	NC	2.60	.3	N318	40	N
262	4080AV	MTV	2.00	.3	N318	40	Y
263	4080AV	MTV	1.70	.3	N318	40	Y
264	4080AV	MTV	1.40	.3	N318	40	N
265	4080AV	MTV	1.70	.3	N318	40	Y
266	4080AV	MTV	1.40	.3	N318	40	N
267	4080AV	MTV	1.70	.3	N318	40	N
268	4080AV	MTV	2.00	.3	N318	40	Y
269	4080AV	MTV	1.70	.3	N318	40	Y
270	4080AV	MTV	1.40	.3	N318	40	N
271	4080AV	MTV	1.70	.3	N318	40	Y

TABLE A-3

IECD EXPANDED IGNITION DIAGNOSTIC TESTS

(Inert Simulant Zone 1 Thickness 1.50 in)

Series 300: NOSOL-363 Propellant

Test Number	Igniter Configuration	Igniter Material	Igniter Mass (g)	δm (g)	Propellant Material	Propellant Mass (g)	Ignition (Yes/No)
301	4080AV	BP	1.8	.5	N363	39.2	N
302	4080AV	BP	2.3	.5	N363	39.2	N
303	4080AV	BP	2.8	.5	N363	39.2	N
304	4080AV	BP	3.3	.5	N363	39.2	N
305	4080AV	BP	3.8	.5	N363	39.2	N
306	4080AV	BP	4.3	.5	N363	39.2	N
307	4080AV	BP	4.8	.5	N363	39.2	Y
308	4080AV	BP	4.3	.5	N363	39.2	N
309	4080AV	BP	4.8	.5	N363	39.2	Y
310	4080AV	BP	4.6	.3	N363	39.2	N
311	4080AV	BP	4.9	.3	N363	39.2	Y
312	4080AV	BP	4.6	.3	N363	39.2	N
313	4080AV	BP	4.9	.3	N363	39.2	N
314	4080AV	BP	5.2	.3	N363	39.2	Y
315	4080AV	BP	4.9	.3	N363	39.2	Y
316	4080AV	BP	4.6	.3	N363	39.2	Y
317	4080AV	BP	4.3	.3	N363	39.2	N
318	4080AV	BP	4.6	.3	N363	39.2	N
319	4080AV	BP	4.9	.3	N363	39.2	Y
320	4080AV	BP	4.6	.3	N363	39.2	N
321	4080AV	BP	4.9	.3	N363	39.2	Y
322	4080AV	BKN	2.5	.5	N363	39.2	Y
323	4080AV	BKN	2.0	.5	N363	39.2	N
324	4080AV	BKN	2.5	.5	N363	39.2	N
325	4080AV	BKN	3.0	.5	N363	39.2	N
326	4080AV	BKN	3.5	.5	N363	39.2	N

Test Number	Igniter Configuration	Material	Mass (g)	δm (g)	Propellant Material	Propellant Mass (g)	Ignition (Yes/No)
327	4080AV	BKN	4.0	.5	N363	39.2	Y
328	4080AV	BKN	3.5	.5	N363	39.2	Y
329	4080AV	BKN	3.0	.3	N363	39.2	Y
330	4080AV	BKN	2.7	.3	N363	39.2	Y
331	4080AV	BKN	2.4	.3	N363	39.2	N
332	4080AV	BKN	2.7	.3	N363	39.2	Y
333	4080AV	BKN	3.4	.3	N363	39.2	No Test
334	4080AV	BKN	2.4	.3	N363	39.2	N
335	4080AV	BKN	2.7	.3	N363	39.2	N
336	4080AV	BKN	3.0	.3	N363	39.2	N
337	4080AV	BKN	3.3	.3	N363	39.2	Y
338	4080AV	BKN	3.0	.3	N363	39.2	N
339	4080AV	BKN	3.3	.3	N363	39.2	Y
340	4080AV	BKN	3.0	.3	N363	39.2	Y
341	4080AV	NC	3.5	.5	N363	39.2	N
342	4080AV	NC	4.0	.5	N363	39.2	Y
343	4080AV	NC	3.5	.5	N363	39.2	N
344	4080AV	NC	4.0	.5	N363	39.2	Y
345	4080AV	NC	3.5	.5	N363	39.2	Y
346	4080AV	NC	3.0	.5	N363	39.2	N
347	4080AV	NC	3.3	.3	N363	39.2	N
348	4080AV	NC	3.6	.3	N363	39.2	N
349	4080AV	NC	3.9	.3	N363	39.2	Y
350	4080AV	NC	3.6	.3	N363	39.2	Y
351	4080AV	NC	3.3	.3	N363	39.2	N
352	4080AV	NC	3.6	.3	N363	39.2	Y
353	4080AV	NC	3.3	.3	N363	39.2	N
354	4080AV	NC	3.6	.3	N363	39.2	Y
355	4080AV	NC	3.3	.3	N363	39.2	N
356	4080AV	NC	3.6	.3	N363	39.2	N

Test Number	Igniter Configuration	Material	Mass (g)	δm (g)	Propellant Material	Mass (g)	Ignition (Yes/No)
357	4080AV	NC	3.9	.3	N363	39.2	Y
358	4080AV	MTV	3.0	.3	N363	40	Y
359	4080AV	MTV	2.7	.3	N363	40	Y
360	4080AV	MTV	2.4	.3	N363	40	N
361	4080AV	MTV	2.7	.3	N363	40	N
362	4080AV	MTV	3.0	.3	N363	40	Y
363	4080AV	MTV	2.7	.3	N363	40	Y
364	4080AV	MTV	2.4	.3	N363	40	N
365	4080AV	MTV	2.7	.3	N363	40	N
366	4080AV	MTV	3.0	.3	N363	40	Y
367	4080AV	MTV	2.7	.3	N363	40	Y

TABLE A-4

IECD EXPANDED IGNITION DIAGNOSTIC TESTS

(Inert Simulant Zone 1 Thickness 1.50 in)

Series 400: LOVA Propellant

Test Number	Igniter Configuration	Igniter Material	Mass (g)	δm (g)	Propellant Material	Propellant Mass (g)	Ignition (Yes/No)
401	4080AV	BP	4.5	.5	LOVA	40	N
402	4080AV	BP	5.0	.5	LOVA	40	N
403	4080AV	BP	5.5	.5	LOVA	40	N
404	4080AV	BP	6.0	.5	LOVA	40	N
405	4080AV	BP	7.0	1.0	LOVA	40	N
406	4080AV	BKN	3.0	1.0	LOVA	40	N
407	4080AV	BKN	4.0	1.0	LOVA	40	N
408	4080AV	BKN	5.0	1.0	LOVA	40	N
409	4080AV	NC	5.0	1.0	LOVA	40	N
410	4080AV	BKN	5.0	1.0	LOVA	51	N
411	5113	BKN	5.0	1.0	LOVA	51	Y
412	5113	BKN	3.0	1.0	LOVA	51	N
413	5113	BKN	4.0	1.0	LOVA	51	N
414	4113-205	BKN	4.0	1.0	LOVA	51	N
415	4113-205	BKN	5.0	1.0	LOVA	51	N
416	5113	BKN	5.0	1.0	LOVA	51	N
417	5113	BKN	6.0	1.0	LOVA	51	Y
418	5113	BKN	5.0	1.0	LOVA	51	Y
419	5113	BKN	4.0	1.0	LOVA	51	Y
420	5113	BKN	2.0	1.0	LOVA	40	N
421	5113	BKN	3.0	1.0	LOVA	40	Y
422	5113	BKN	4.0	1.0	LOVA	40	Y
423	5113	BKN	3.0	1.0	LOVA	40	Y
424	5113	BKN	2.5	1.0	LOVA	40	Y
425	5113	BKN	2.5	1.0	LOVA	40	Y
426	5113	BKN	3.0	1.0	LOVA	40	Y
427	5113	BKN	4.0	1.0	LOVA	40	Y
428	5113	BKN	2.5	1.0	LOVA	40	Y
429	5113	BKN	3.0	1.0	LOVA	40	Y

Test Number	Igniter Configuration	Material	Mass (g)	δm (g)	Propellant Material	Propellant Mass (g)	Ignition (Yes/No)
430	5113	BKN	2.5	.5	LOVA	40	N
431	5113	BKN	3.0	.5	LOVA	40	Y
432	5113	BKN	2.5	.5	LOVA	40	Y
433	5113	BKN	2.0	.5	LOVA	40	N
434	5113	BKN	2.5	.5	LOVA	40	N
435	5113	BKN	3.0	.5	LOVA	40	Y
436	5113	BKN	2.5	.5	LOVA	40	Y
437	5113	BKN	2.0	.5	LOVA	40	N
438	5113	BKN	2.5	.5	LOVA	40	N
439	5113	BKN	3.0	.5	LOVA	40	Y
440	5113	BP	6.0	1.0	LOVA	40	N
441	5113	BP	7.0	1.0	LOVA	40	Y
442	5113	BP	6.0	1.0	LOVA	40	Y
443	5113	BP	5.0	1.0	LOVA	40	Y
444	5113	BP	4.0	1.0	LOVA	40	N
445	5113	BP	5.0	1.0	LOVA	40	N
446	5113	BP	6.0	1.0	LOVA	40	N
447	5113	BP	7.0	1.0	LOVA	40	Y
448	5113	BP	6.0	1.0	LOVA	40	Y
449	5113	BP	5.0	1.0	LOVA	40	Y
450	5113	MTV	3.0	0.5	LOVA	40	N
451	5113	MTV	3.5	0.5	LOVA	40	Y
452	5113	MTV	3.0	0.5	LOVA	40	Y
453	5113	MTV	2.5	0.5	LOVA	40	N
454	5113	MTV	3.0	0.5	LOVA	40	Y
455	5113	MTV	2.5	0.5	LOVA	40	N
456	5113	MTV	3.0	0.5	LOVA	40	N
457	5113	MTV	3.5	0.5	LOVA	40	Y
458	5113	MTV	3.0	0.5	LOVA	40	Y
459	5113	MTV	2.5	0.5	LOVA	40	N
460	5113	NC	4.0	0.5	LOVA	40	N
461	5113	NC	5.0	0.5	LOVA	40	Y

Test Number	Igniter Configuration	Material	Mass (g)	δm (g)	Propellant Material	Propellant Mass (g)	Ignition (Yes/No)
462	5113	NC	4.0	0.5	LOVA	40	Y
463	5113	NC	3.0	0.5	LOVA	40	N
464	5113	NC	4.0	0.5	LOVA	40	N
465	5113	NC	5.0	0.5	LOVA	40	Y
466	5113	NC	4.0	0.5	LOVA	40	N
467	5113	NC	5.0	0.5	LOVA	40	Y
468	5113	NC	4.0	0.5	LOVA	40	N
469	5113	NC	5.0	0.5	LOVA	40	Y

APPENDIX B

IECD DATA REDUCTION

Propellant	BP	$BKNO_3$	MTV	NC	$BMoO_3$
NACO	x	x	x	x	x
NOSOL-318	x	x	x	x	
NOSOL-363	x	x	x	x	
LOVA	x	x	x	x	

1. Igniter Calibration Data with Baseline Igniter
2. 50% Firepoint Results: Mass Distribution (g)
3. 50% Firepoint Results: Energy Distribution (cal)

TABLE B-1

IECD DATA REDUCTION: BP/NACO

	Igniter				Propellant				
Test Number	Matl	Mass (g)	Matl	Ignition (Yes/No)	P_{20} (psi)	P_{21} (psi)	P_{2max} (psi)	τ_{ign} (ms)	τ_{peak} (ms)
115	BP	1.2	NACO	N	120	-	-	-	-
116	BP	1.5	NACO	N	210	-	-	-	-
117	BP	1.8	NACO	N	320	-	-	-	-
118	BP	2.1	NACO	Y	340	NFR	-	-	-
119	BP	1.8	NACO	Y	320	15	3450	2100	2200
120	BP	1.5	NACO	N	250	-	-	-	-
121	BP	1.8	NACO	Y	320	15	2250	2240	2320
122	BP	1.5	NACO	Y	210	15	3110	2500	2590
123	BP	1.2	NACO	N	120	-	-	-	-

Fifty percent firepoint $\overline{m} = 1.65 \pm .26$

NFR ~ No Film Record

TABLE B-2

IECD DATA REDUCTION: BKN/NACO

	Igniter				Propellant				
Test Number	Matl	Mass (g)	Matl	Ignition (Yes/No)	P_{20} (psi)	P_{21} (psi)	P_{2max} (psi)	τ_{ign} (ms)	τ_{peak} (ms)
124	BKN	.8	NACO	Y	100	NFR	-	-	-
125	BKN	.6	NACO	N	80	-	-	-	-
126	BKN	.8	NACO	N	100	-	-	-	-
127	BKN	1.0	NACO	N	120	-	-	-	-
128	BKN	1.2	NACO	Y	280	15	2750	1260	1290
129	BKN	1.0	NACO	Y	130	15	3350	1660	1750
130	BKN	.8	NACO	N	100	-	-	-	-
131	BKN	1.0	NACO	Y	120	15	2700	1580	1700
132	BKN	.8	NACO	Y	100	15	1800	2420	2530

Fifty percent firepoint $\overline{m} = 0.90 \pm .17$

TABLE B-3

IECD DATA REDUCTION: NC/NACO

	Igniter			Propellant					
Test Number	Matl	Mass (g)	Matl	Ignition (Yes/No)	P_{20} (psi)	P_{21} (psi)	P_{2max} (psi)	τ_{ign} (ms)	τ_{peak} (ms)
133	NC	1.4	NACO	N	50	-	-	-	-
134	NC	1.7	NACO	N	90	-	-	-	-
135	NC	2.0	NACO	N	100	-	-	-	-
136	NC	2.3	NACO	N	110	-	-	-	-
137	NC	2.6	NACO	Y	140	P_{20}	3520	30	80
138	NC	2.3	NACO	Y	100	15	2350	3680	3720
139	NC	2.0	NACO	N	100	-	-	-	-
140	NC	2.3	NACO	Y	100	P_{20}	2550	40	90
141	NC	2.0	NACO	N	90	-	-	-	-
142	NC	2.3	NACO	N	100	-	-	-	-
143	NC	2.6	NACO	N	110	-	-	-	-
144	NC	2.9	NACO	Y	160	P_{20}	1900	30	90

Fifty percent firepoint $\bar{m} = 2.38 \pm .35$

TABLE B-4

IECD DATA REDUCTION: MTV/NACO

	Igniter				Propellant				
Test Number	Matl	Mass (g)	Matl	Ignition (Yes/No)	P_{20} (psi)	P_{21} (psi)	P_{2max} (psi)	τ_{ign} (ms)	τ_{peak} (ms)
147	MTV	1.7	NACO	Y	400	15	3400	30	65
148	MTV	1.4	NACO	Y	300	200	3500	15	60
149	MTV	1.1	NACO	N	200	-	-	-	-
150	MTV	1.4	NACO	Y	250	15	3400	25	60
151	MTV	1.1	NACO	N	200	-	-	-	-
152	MTV	1.4	NACO	Y	250	150	3300	20	55
153	MTV	1.1	NACO	Y	150	15	NFR	2000+	2000+
154	MTV	0.8	NACO	N	100	-	-	-	-
155	MTV	1.1	NACO	Y	200	15	NFR	3000+	3000+
156	MTV	0.8	NACO	N	100	-	-	-	-

Fifty percent firepoint $\overline{m} = 1.10 \pm .14$

TABLE B-5

IECD DATA REDUCTION: BMO/NACO

	Igniter				Propellant				
Test Number	Matl	Mass (g)	Matl	Ignition (Yes/No)	P_{20} (psi)	P_{21} (psi)	P_{2max} (psi)	τ_{ign} (ms)	τ_{peak} (ms)
161	BMO	5.0	NACO	N	50	-	-	-	-
162	BMO	5.5	NACO	N	50	-	-	-	-
163	BMO	6.0	NACO	Y	75	15	NFR	5000+	5000+
164	BMO	5.5	NACO	Y	50	15	2400	2880	3020
165	BMO	5.0	NACO	N	50	-	-	-	-
166	BMO	5.5	NACO	Y	50	15	3600	2050	2200
167	BMO	5.0	NACO	N	50	-	-	-	-
168	BMO	5.5	NACO	N	50	-	-	-	-
169	BMO	6.0	NACO	N	50	-	-	-	-
170	BMO	6.5	NACO	Y	50	15	NFR	5000+	5000+
171	BMO	6.0	NACO	N	50	-	-	-	-
172	BMO	6.5	NACO	N	50	-	-	-	-

Fifty percent firepoint $\overline{m}$ = 5.75±.67

TABLE B-6

IECD DATA REDUCTION: BP/N318

	Igniter				Propellant				
Test Number	Matl	Mass (g)	Matl	Ignition (Yes/No)	P_{20} (psi)	P_{21} (psi)	P_{2max} (psi)	τ_{ign} (ms)	τ_{peak} (ms)
218	BP	4.7	N318	N	1100	-	-	-	-
219	BP	5.0	N318	Y	1200	700	600	10	35
220	BP	4.7	N318	Y	1200	750	600	5	45
221	BP	4.4	N318	N	1300	-	-	-	-
222	BP	4.7	N318	Y	1300	600	500	10	75
223	BP	4.4	N318	N	1200	-	-	-	-
224	BP	4.7	N318	Y	1350	400	650	15	80
225	BP	4.4	N318	Y	1200	500	1100	40	210
226	BP	4.1	N318	Y	1100	900	1600	25	155
227	BP	3.8	N318	Y	900	15	NFR	5000+	5000+
228	BP	3.5	N318	N	1100	-	-	-	-
229	BP	3.8	N318	Y	1100	15	NFR	9000+	9000+

Fifty percent firepoint $\overline{m}$ = 4.40±1.1

TABLE B-7

IECD DATA REDUCTION: BKN/N318

	Igniter				Propellant				
Test Number	Matl	Mass (g)	Matl	Ignition (Yes/No)	P_{20} (psi)	P_{21} (psi)	P_{2max} (psi)	τ_{ign} (ms)	τ_{peak} (ms)
233	BKN	2.5	N318	Y	700	15	NFR	6000+	6000+
234	BKN	2.3	N318	Y	700	15	NFR	5000+	5000+
235	BKN	2.1	N318	Y	600	15	NFR	6000+	6000+
236	BKN	1.9	N318	N	400	-	-	-	-
237	BKN	2.1	N318	Y	500	15	700	9200	9350
238	BKN	1.9	N318	Y	500	15	NFR	10000+	10000+
239	BKN	1.7	N318	N	300	-	-	-	-
240	BKN	1.9	N318	Y	400	15	300	6150	6250
241	BKN	1.7	N318	N	300	-	-	-	-
242	BKN	1.9	N318	Y	400	15	1100	6050	6180
243	BKN	1.7	N318	Y	350	15	1500	6400	6520
244	BKN	1.5	N318	N	250	-	-	-	-
•245	BKN	1.7	N318	Y	400	15	700	7400	7550

Fifty percent firepoint $\overline{m} = 1.8 \pm .17$

TABLE B-8

IECD DATA REDUCTION: NC/N318

	Igniter				Propellant				
Test Number	Matl	Mass (g)	Matl	Ignition (Yes/No)	P_{20} (psi)	P_{21} (psi)	P_{2max} (psi)	τ_{ign} (ms)	τ_{peak} (ms)
250	NC	2.3	N318	N	50	-	-	-	-
251	NC	2.6	N318	N	75	-	-	-	-
252	NC	2.9	N318	N	100	-	-	-	-
253	NC	3.2	N318	Y	150	NFR	-	-	-
254	NC	2.9	N318	N	75	-	-	-	-
255	NC	3.2	N318	Y	150	P_{20}	1500	15	25
256	NC	2.9	N318	N	125	-	-	-	-
257	NC	3.2	N318	N	150	-	-	-	-
258	NC	3.5	N318	Y	150	15	NFR	7000+	7000+
259	NC	3.2	N318	Y	150	P_{20}	1650	10	15
260	NC	2.9	N318	Y	100	15	NFR	10000+	10000+
261	NC	2.6	N318	N	100	-	-	-	-

Fifty percent firepoint $\overline{m} = 3.05 \pm .21$

TABLE B-9

IECD DATA REDUCTION MTV/N318

	Igniter				Propellant				
Test Number	Matl	Mass (g)	Matl	Ignition (Yes/No)	P_{20} (psi)	P_{21} (psi)	P_{2max} (psi)	τ_{ign} (ms)	τ_{peak} (ms)
262	MTV	2.0	N318	Y	300	15	NFR	6000+	6000+
263	MTV	1.7	N318	Y	500	15	1400	5010	5100
264	MTV	1.4	N318	N	350	-	-	-	-
265	MTV	1.7	N318	Y	300	15	1500	4550	4620
266	MTV	1.4	N318	N	200	-	-	-	-
267	MTV	1.7	N318	N	350	-	-	-	-
268	MTV	2.0	N318	Y	400	15	2450	5750	5900
269	MTV	1.7	N318	Y	400	15	1500	5650	5710
270	MTV	1.4	N318	N	300	-	-	-	-
271	MTV	1.7	N318	Y	400	15	1750	4600	4710

Fifty percent firepoint $\overline{m} = 1.63 \pm .10$

TABLE B-10

IECD DATA REDUCTION: BP/N363

	Igniter				Propellant				
Test Number	Matl	Mass (g)	Matl	Ignition (Yes/No)	P_{20} (psi)	P_{21} (psi)	P_{2max} (psi)	τ_{ign} (ms)	τ_{peak} (ms)
310	BP	4.6	N363	N	1100	-	-	-	-
311	BP	4.9	N363	Y	1250	50	1700	80	110
312	BP	4.6	N363	N	1000	-	-	-	-
313	BP	4.9	N363	N	1100	-	-	-	-
314	BP	5.2	N363	Y	1750	NFR	-	-	-
315	BP	4.9	N363	Y	1750	250	500	40	60
316	BP	4.6	N363	Y	1100	50	800	50	125
317	BP	4.3	N363	N	1000	-	-	-	-
318	BP	4.6	N363	N	1400	-	-	-	-
319	BP	4.9	N363	Y	1500	15	NFR	3500+	3500+
320	BP	4.6	N363	N	1250	-	-	-	-
321	BP	4.9	N363	Y	1500	100	600	70	105

Fifty percent firepoint $\overline{m} = 4.75 \pm .18$

TABLE B-11

IECD DATA REDUCTION: BKN/N363

Test Number	Igniter Matl	Igniter Mass (g)	Propellant Matl	Ignition (Yes/No)	P_{20} (psi)	P_{21} (psi)	P_{2max} (psi)	τ_{ign} (ms)	τ_{peak} (ms)
329	BKN	3.0	N363	Y	850	15	2100	30	140
330	BKN	2.7	N363	Y	850	15	NFR	6000+	6000+
331	BKN	2.4	N363	N	550	-	-	-	-
332	BKN	2.7	N363	Y	750	15	1750	40	150
333	No Test								
334	BKN	2.4	N363	N	600	-	-	-	-
335	BKN	2.7	N363	N	800	-	-	-	-
336	BKN	3.0	N363	N	900	-	-	-	-
337	BKN	3.3	N363	Y	1100	15	1100	25	100
338	BKN	3.0	N363	N	1000	-	-	-	-
339	BKN	3.3	N363	Y	1100	15	NFR	7000+	7000+
340	BKN	3.0	N363	Y	1300	15	NFR	5000+	5000+

Fifty percent firepoint $\overline{m} = 2.85 \pm .40$

TABLE B-12

IECD DATA REDUCTION: NC/N363

	Igniter				Propellant				
Test Number	Matl	Mass (g)	Matl	Ignition (Yes/No)	P_{20} (psi)	P_{21} (psi)	P_{2max} (psi)	τ_{ign} (ms)	τ_{peak} (ms)
347	NC	3.3	N363	N	1300	-	-	-	-
348	NC	3.6	N363	N	1900	-	-	-	-
349	NC	3.9	N363	Y	1900	15	850	30	110
350	NC	3.6	N363	Y	1800	15	600	30	140
351	NC	3.3	N363	N	1400	-	-	-	-
352	NC	3.6	N363	Y	1900	15	1500	30	65
353	NC	3.3	N363	N	1300	-	-	-	-
354	NC	3.6	N363	Y	1800	15	1600	30	120
355	NC	3.3	N363	N	1250	-	-	-	-
356	NC	3.6	N363	N	1900	-	-	-	-
357	NC	3.9	N363	Y	2100	15	600	30	80

Fifty percent firepoint $\overline{m} = 3.57 \pm .13$

TABLE B-13

IECD DATA REDUCTION: MTV/N363

	Igniter			Propellant					
Test Number	Matl	Mass (g)	Matl	Ignition (Yes/No)	P_{20} (psi)	P_{21} (psi)	P_{2max} (psi)	τ_{ign} (ms)	τ_{peak} (ms)
358	MTV	3.0	N363	Y	800	15	2500	4700	4850
359	MTV	2.7	N363	Y	500	15	650	7500	7750
360	MTV	2.4	N363	N	600	-	-	-	-
361	MTV	2.7	N363	N	750	-	-	-	-
362	MTV	3.0	N363	Y	850	450	2600	40	100
363	MTV	2.7	N363	Y	600	100	1400	50	120
364	MTV	2.4	N363	N	600	-	-	-	-
365	MTV	2.7	N363	N	700	-	-	-	-
366	MTV	3.0	N363	Y	800	100	2100	50	140
367	MTV	2.7	N363	Y	650	400	3200	40	90

Fifty percent firepoint $\overline{m} = 2.70 \pm .14$

TABLE B-14

IECD DATA REDUCTION: BKN/LOVA

	Igniter				Propellant				
Test Number	Matl	Mass (g)	Matl	Ignition (Yes/No)	P_{20} (psi)	P_{21} (psi)	P_{2max} (psi)	τ_{ign} (ms)	τ_{peak} (ms)
430	BKN	2.5	LOVA	N	1200	-	-	-	-
431	BKN	3.0	LOVA	Y	1800	1200	3700	25	105
432	BKN	2.5	LOVA	Y	1400	400	2400	40	145
433	BKN	2.0	LOVA	N	800	-	-	-	-
434	BKN	2.5	LOVA	N	1400	-	-	-	-
435	BKN	3.0	LOVA	Y	1800	1400	5000	30	95
436	BKN	2.5	LOVA	Y	1400	1000	4200	20	125
437	BKN	2.0	LOVA	N	800	-	-	-	-
438	BKN	2.5	LOVA	N	1200	-	-	-	-
439	BKN	3.0	LOVA	Y	1800	1500	4800	25	90

Fifty percent firepoint $\overline{m} = 2.55 \pm .22$

TABLE B-15

IECD DATA REDUCTION: BP/LOVA

	Igniter				Propellant				
Test Number	Matl	Mass (g)	Matl	Ignition (Yes/No)	P_{20} (psi)	P_{21} (psi)	P_{2max} (psi)	τ_{ign} (ms)	τ_{peak} (ms)
440	BP	6.0	LOVA	N	2400	-	-	-	-
441	BP	7.0	LOVA	Y	3000	2200	6800	15	55
442	BP	6.0	LOVA	Y	2600	1800	3200	30	100
443	BP	5.0	LOVA	Y	1800	1300	3200	20	110
444	NP	4.0	LOVA	N	1200	-	-	-	-
445	BP	5.0	LOVA	N	2000	-	-	-	-
446	BP	6.0	LOVA	N	2400	-	-	-	-
447	BP	7.0	LOVA	Y	2800	2400	2400	15	70
448	BP	6.0	LOVA	Y	2600	1800	3600	25	100
449	BP	5.0	LOVA	Y	2000	1600	7600	15	75

Fifty percent firepoint $\overline{m}$ - 5.75±1.16

TABLE B-16

IECD DATA REDUCTION: MTV/LOVA

	Igniter				Propellant				
Test Number	Matl	Mass (g)	Matl	Ignition (Yes/No)	P_{20} (psi)	P_{21} (psi)	P_{2max} (psi)	τ_{ign} (ms)	τ_{peak} (ms)
450	MTV	3.0	LOVA	N	1000	-	-	-	-
451	MTV	3.5	LOVA	Y	1100	1000	3100	25	105
452	MTV	3.0	LOVA	Y	1000	P_{20}	7800	10	100
453	MTV	2.5	LOVA	N	600	-	-	-	-
454	MTV	3.0	LOVA	Y	1000	600	3000	40	155
455	MTV	2.5	LOVA	N	800	-	-	-	-
456	MTV	3.0	LOVA	N	900	-	-	-	-
457	MTV	3.5	LOVA	Y	900	800	6500	15	80
458	MTV	3.0	LOVA	Y	900	900	3000	15	140
459	MTV	2.5	LOVA	N	700	-	-	-	-

Fifty percent firepoint $\overline{m} = 2.95 \pm .22$

TABLE B-17

IECD DATA REDUCTION: NC/LOVA

	Igniter				Propellant				
Test Number	Matl	Mass (g)	Matl	Ignition (Yes/No)	P_{20} (psi)	P_{21} (psi)	P_{2max} (psi)	τ_{ign} (ms)	τ_{peak} (ms)
460	NC	4.0	LOVA	N	1200	-	-	-	-
461	NC	5.0	LOVA	Y	4000	2500	3100	60	80
462	NC	4.0	LOVA	Y	2100	1200	2000	40	100
463	NC	3.0	LOVA	N	200	-	-	-	-
464	NC	4.0	LOVA	N	2100	-	-	-	-
465	NC	5.0	LOVA	Y	3600	3200	6200	15	50
466	NC	4.0	LOVA	N	1200	-	-	-	-
467	NC	5.0	LOVA	Y	3600	2900	3200	15	55
468	NC	4.0	LOVA	N	1200	-	-	-	-
469	NC	5.0	LOVA	Y	3800	3500	7000	10	50

Fifty percent firepoint $\overline{m} = 4.30 \pm .31$

TABLE B-18

IGNITER CALIBRATION DATA WITH BASELINE IGNITER

Test	Material	M-Mass (g)	P_{max} (psi)	$\tau_{p_{max}}$ (ms)	τ_{final} (ms)	$\frac{\Delta p_{max}}{\Delta \tau_{p_{max}}}$ (psi/ms)	P_{max}/m (psi/g)	$\dot{P}_{max}/m$ (psi/ms-g)
35	BP	1	1240	2.2	8	564	1240	564
26	BP	2	3060	2	8	1530	1530	765
4-8	BP	3.5	5200	1.8	5.3	2890	1485	825
5-8	BP	6.0	9400	1.6	5.3	5875	1565	979
38	$BKNO_3$	1	1500	1	7.2	1500	1500	1500
52	$BKNO_3$	2.0	3100	1.4	7.2	2200	1550	1100
6-8	$BKNO_3$	3	4800	1.2	7.0	4000	1600	1335
010B	NC	1	1700	10	16	170	1700	170
006	NC	2	3400	7	12	283	1700	142
3-8	NC	3.5	12000	3	6	4000	3400	1143
7-8	NC	4.5	16100	2.8	5.2	5750	3580	1277
1-8	MTV	1	800	.5	3.5	1600	1600	1600
2-8	MTV	2.5	1400	.6	4.6	2330	560	932
8-8	MTV	3.5	1800	.6	3.2	3000	514	857
5-8	$BMoO_3$	5.75	800	.4	6	1000	90	175

TABLE B-19

50% FIREPOINT RESULTS:

MASS DISTRIBUTION (g)

	IGNITER MATERIAL				
Propellant	BP	BKN	NC	MTV	$BMoO_3$
NACO	1.65	.90	2.38	1.10	5.75
N318	4.40	1.80	3.05	1.63	-
N363	4.75	2.85	3.57	2.70	-
LOVA	5.75	2.55	4.30	2.95	-

TABLE B-20

50% FIREPOINT RESULTS:

ENERGY DISTRIBUTION (cal)

	IGNITER MATERIAL				
Propellant	BP	BKN	NC	MTV	$BMoO_3$
NACO	1130	1350	2300	1595	2875
N318	3010	2700	2940	2360	-
N363	3250	4280	3450	3900	-
LOVA	3933	3825	4150	4280	-

APPENDIX C

BRUCETON METHOD COMPUTATIONS FOR CALCULATING 50% FIREPOINT

APPLIED COMBUSTION TECHNOLOGY

IECD IGNITION EFFECTIVENESS TESTS

BRUCETON METHOD OF DETERMINING
50% FIRE POINT

DATE MARCH 1982
IGNITER-BLACK POWDER
PROPELLANT-NACO

MEAN- 1.65 STD DEV-0.257

MASS (G)	NUMBER OF FIRES	NUMBER OF NO FIRES
1.20	0	2
1.50	1	2
1.80	2	1
2.10	1	0
TOTAL	4	5

APPLIED COMBUSTION TECHNOLOGY

IECD IGNITION EFFECTIVENESS TESTS

BRUCETON METHOD OF DETERMINING
50% FIRE POINT

DATE MARCH 1982
IGNITER-BKNO3
PROPELLANT-NACO

MEAN- 0.90 STD DEV-0.171

MASS (G)	NUMBER OF FIRES	NUMBER OF NO FIRES
0.60	0	1
0.80	2	2
1.00	2	1
1.20	1	0
TOTAL	5	4

APPLIED COMBUSTION TECHNOLOGY

IECD IGNITION EFFECTIVENESS TESTS

BRUCETON METHOD OF DETERMINING
50% FIRE POINT

DATE MARCH 1982
IGNITER-NITROCELLULOSE
PROPELLANT-NACO

MEAN- 2.38 STD DEV-0.348

MASS (G)	NUMBER OF FIRES	NUMBER OF NO FIRES
1.40	0	1
1.70	0	1
2.00	0	3
2.30	2	2
2.60	1	1
2.90	1	0
TOTAL	4	8

APPLIED COMBUSTION TECHNOLOGY

IECD IGNITION EFFECTIVENESS TESTS

BRUCETON METHOD OF DETERMINING
50% FIRE POINT

DATE JUNE 82
IGNITER-MTV
PROPELLANT-NACO

MEAN- 1.10 STD DEV-0.136

MASS (G)	NUMBER OF FIRES	NUMBER OF NO FIRES
0.80	0	2
1.10	2	2
1.40	3	0
1.70	1	0
TOTAL	6	4

APPLIED COMBUSTION TECHNOLOGY

IECD IGNITION EFFECTIVENESS TESTS

BRUCETON METHOD OF DETERMINING
50% FIRE POINT

DATE JUNE 82
IGNITER-BMO03
PROPELLANT-NACO

MEAN- 5.75   STD DEV-0.671

MASS (G)	NUMBER OF FIRES	NUMBER OF NO FIRES
5.00	0	3
5.50	2	2
6.00	1	2
6.50	2	0
TOTAL	5	7

APPLIED COMBUSTION TECHNOLOGY

IECD IGNITION EFFECTIVENESS TESTS

BRUCETON METHOD OF DETERMINING
50% FIRE POINT

DATE MARCH 82
IGNITER-BLACK POWDER
PROPELLANT-NOSOL-318

MEAN- 4.40 STD DEV-1.108

MASS (G)	NUMBER OF FIRES	NUMBER OF NO FIRES
3.50	0	1
3.80	2	0
4.10	1	0
4.40	1	2
4.70	3	1
5.00	1	0
TOTAL	8	4

APPLIED COMBUSTION TECHNOLOGY

IECD IGNITION EFFECTIVENESS TESTS

BRUCETON METHOD OF DETERMINING
50% FIRE POINT

DATE MARCH 82
IGNITER-BKNO3
PROPELLANT-NOSOL-318

MEAN- 1.80 STD DEV-0.171

MASS (G)	NUMBER OF FIRES	NUMBER OF NO FIRES
1.50	0	1
1.70	2	2
1.90	3	1
2.10	2	0
2.30	1	0
2.50	1	0
TOTAL	9	4

APPLIED COMBUSTION TECHNOLOGY

IECD IGNITION EFFECTIVENESS TESTS

BRUCETON METHOD OF DETERMINING
50% FIRE POINT

DATE MARCH 82
IGNITER-NITROCELLULOSE
PROPELLANT-NOSOL-318

MEAN- 3.05 STD DEV-0.208

MASS (G)	NUMBER OF FIRES	NUMBER OF NO FIRES
2.30	0	1
2.60	0	2
2.90	1	3
3.20	3	1
3.50	1	0
TOTAL	5	7

APPLIED COMBUSTION TECHNOLOGY

IECD IGNITION EFFECTIVENESS TESTS

BRUCETON METHOD OF DETERMINING
50% FIRE POINT

DATE JUNE 82
IGNITER-MTV
PROPELLANT-NOSOL-318

MEAN- 1.63 STD DEV-0.105

MASS (G)	NUMBER OF FIRES	NUMBER OF NO FIRES
1.40	0	3
1.70	4	1
2.00	2	0
TOTAL	6	4

APPLIED COMBUSTION TECHNOLOGY

IECD IGNITION EFFECTIVENESS TESTS

BRUCETON METHOD OF DETERMINING
50% FIRE POINT

DATE APRIL 82
IGNITER-BLACK POWDER
PROPELLANT-NOSOL 363

MEAN- 4.75 STD DEV-0.176

MASS (G)	NUMBER OF FIRES	NUMBER OF NO FIRES
4.30	0	1
4.60	1	4
4.90	4	1
5.20	1	0
TOTAL	6	6

APPLIED COMBUSTION TECHNOLOGY
IECD IGNITION EFFECTIVENESS TESTS

BRUCETON METHOD OF DETERMINING
50% FIRE POINT

DATE APRIL 82
IGNITER-BKNO3
PROPELLANT-NOSOL 363

MEAN- 2.85 STD DEV-0.403

MASS (G)	NUMBER OF FIRES	NUMBER OF NO FIRES
2.40	0	2
2.70	2	1
3.00	2	2
3.30	2	0
TOTAL	6	5

APPLIED COMBUSTION TECHNOLOGY

IECD IGNITION EFFECTIVENESS TESTS

BRUCETON METHOD OF DETERMINING
50% FIRE POINT

DATE APRIL 82
IGNITER-NITROCELLULOSE
PROPELLANT-NOSOL 363

MEAN- 3.57 STD DEV-0.131

MASS (G)	NUMBER OF FIRES	NUMBER OF NO FIRES
3.30	0	4
3.60	3	2
3.90	2	0
TOTAL	5	6

APPLIED COMBUSTION TECHNOLOGY

IECD IGNITION EFFECTIVENESS TESTS

BRUCETON METHOD OF DETERMINING
50% FIRE POINT

DATE JUNE 82
IGNITER-MTV
PROPELLANT-NOSOL-363

MEAN- 2.70 STD DEV-0.136

MASS (G)	NUMBER OF FIRES	NUMBER OF NO FIRES
2.40	0	2
2.70	3	2
3.00	3	0
TOTAL	6	4

APPLIED COMBUSTION TECHNOLOGY

IECD IGNITION EFFECTIVENESS TESTS

BRUCETON METHOD OF DETERMINING
50% FIRE POINT

DATE JULY 82
IGNITER-BP
PROPELLANT-LOVA

MEAN- 5.75 STD DEV-1.161

MASS (G)	NUMBER OF FIRES	NUMBER OF NO FIRES
4.00	0	1
5.00	2	1
6.00	2	2
7.00	2	0
TOTAL	6	4

APPLIED COMBUSTION TECHNOLOGY

IECD IGNITION EFFECTIVENESS TESTS

BRUCETON METHOD OF DETERMINING
50% FIRE POINT

DATE JULY 82
IGNITER-BK 03
PROPELLANT-LOVA

MEAN- 2.55 STD DEV-0.218

MASS (G)	NUMBER OF FIRES	NUMBER OF NO FIRES
2.00	0	2
2.50	2	3
3.00	3	0
TOTAL	5	5

APPLIED COMBUSTION TECHNOLOGY

IECD IGNITION EFFECTIVENESS TESTS

BRUCETON METHOD OF DETERMINING
50% FIRE POINT

DATE JULY 82
IGNITER-NC
PROPELLANT-LOVA

MEAN- 4.30 STD DEV-0.306

MASS (G)	NUMBER OF FIRES	NUMBER OF NO FIRES
3.00	0	1
4.00	1	4
5.00	4	0
TOTAL	5	5

APPLIED COMBUSTION TECHNOLOGY

IECD IGNITION EFFECTIVENESS TESTS

BRUCETON METHOD OF DETERMINING
50% FIRE POINT

DATE JULY 82
IGNITER-MTV
PROPELLANT-LOVA

MEAN- 2.95 STD DEV-0.218

MASS (G)	NUMBER OF FIRES	NUMBER OF NO FIRES
2.50	0	3
3.00	3	2
3.50	2	0
TOTAL	5	5

APPENDIX D

IECD DATA ANALYSIS WORKING CURVES

Data Analysis

Igniter calibration data have been combined with the analytical model to generate a set of working curves to facilitate data reduction of the IECD ignition effectiveness test results. To provide a common basis for presenting the ignition data, it was decided to evaluate the igniter performance at peak conditions, e.g., peak pressure, peak energy flux, etc. These working curves are presented in this section.

Igniter calibration data were generated for BP, $BKNO_3$, NC, and MTV over the range of igniter mass loadings utilized in the IECD ignition effectiveness test series. Peak igniter pressure (P_c) data and average pressurization rate (dP_c/dt) data are presented in Figures D-1 through D-4, respectively for BP, $BKNO_3$, NC, and MTV. Using the igniter analytical model, igniter mass generation rates, $\dot{m}_s$, gas phase flow rates, $\dot{m}_g$, and condensed phase flow rates, $\dot{m}_g$, were generated for each igniter material tested over a β-value range from 0 to 0.8; these results are shown in Figures D-5 through D-9 as a function of igniter pressure. Gas phase and condensed phase energy fluxes as a function of mass flow rate are presented in Figures D-10 and D-11, respectively.

Total energy into the bed and total energy flux into the bed have been expressed in terms of igniter mass loading in Figures D-12 and D-13, respectively. The procedure for using these curves for any particular IECD ignition effectiveness test is as follows:

1. Test Number
2. Propellant
3. Igniter Material Type
4. Igniter Material Mass (g)
5. Igniter Vent Configuration

6. Peak Pressure (P_c) as function of igniter mass: Figures D-1 to D-4
7. Gas phase flow rate ($\dot{m}_g$) as function of P_c: Figures D-5 to D-8
8. Mass generation rate ($\dot{m}_s$) as function of P_c: Figures D-5 to D-8
9. Determine β from Nasa Lewis Code at P_c
10. Condesned phase flow rate ($\dot{m}_{cp}$) as function of $\dot{m}_s$, β: Figure D-9
11. Gas phase energy flux ($\dot{E}_g$) as function of $\dot{m}_g$: Figure D-10
12. Condensed phase energy flux ($\dot{E}_{cp}$) function of $\dot{m}_{cp}$: Figure D-11
13. Total energy into bed E_{tot}) as function of mass: Figure D-12
14. Total energy flux into bed ($\dot{E}_{tot}$) as function of mass: Figure D-13

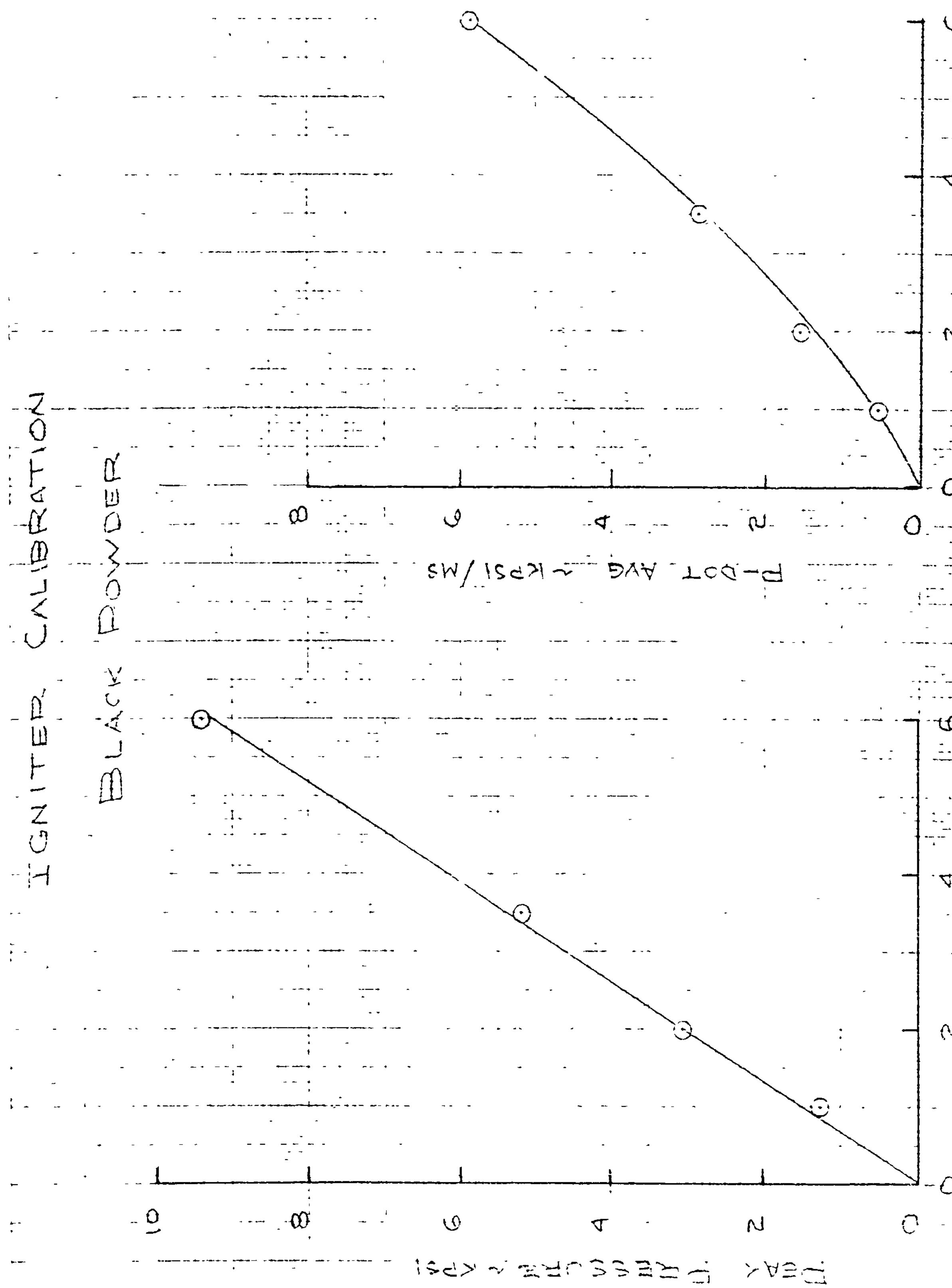

Figure D-1 Igniter Calibration Data: BP

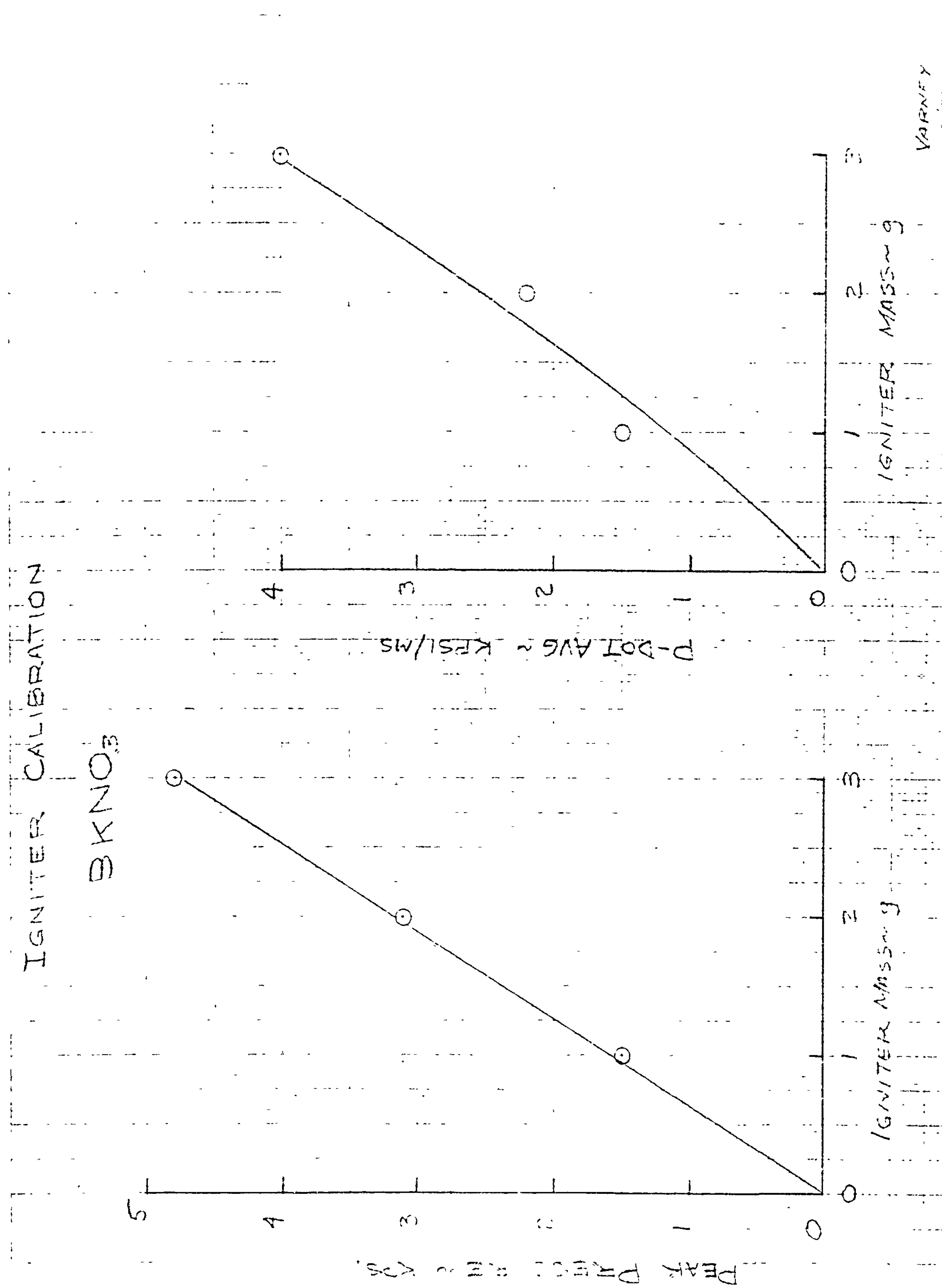

Figure D-2 Igniter Calibration Data: $BKNO_3$

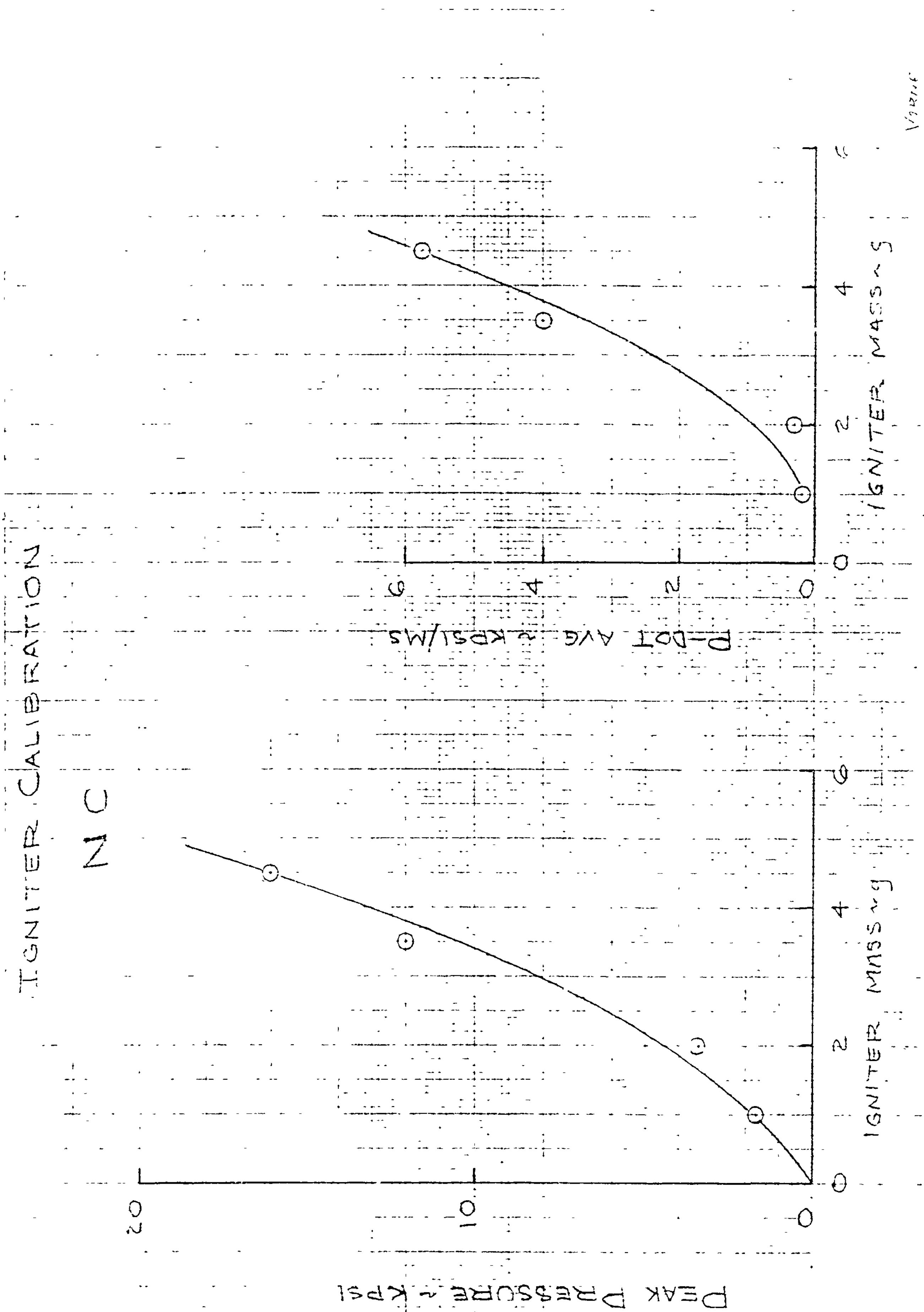

Figure D-3 Igniter Calibration Data: NC

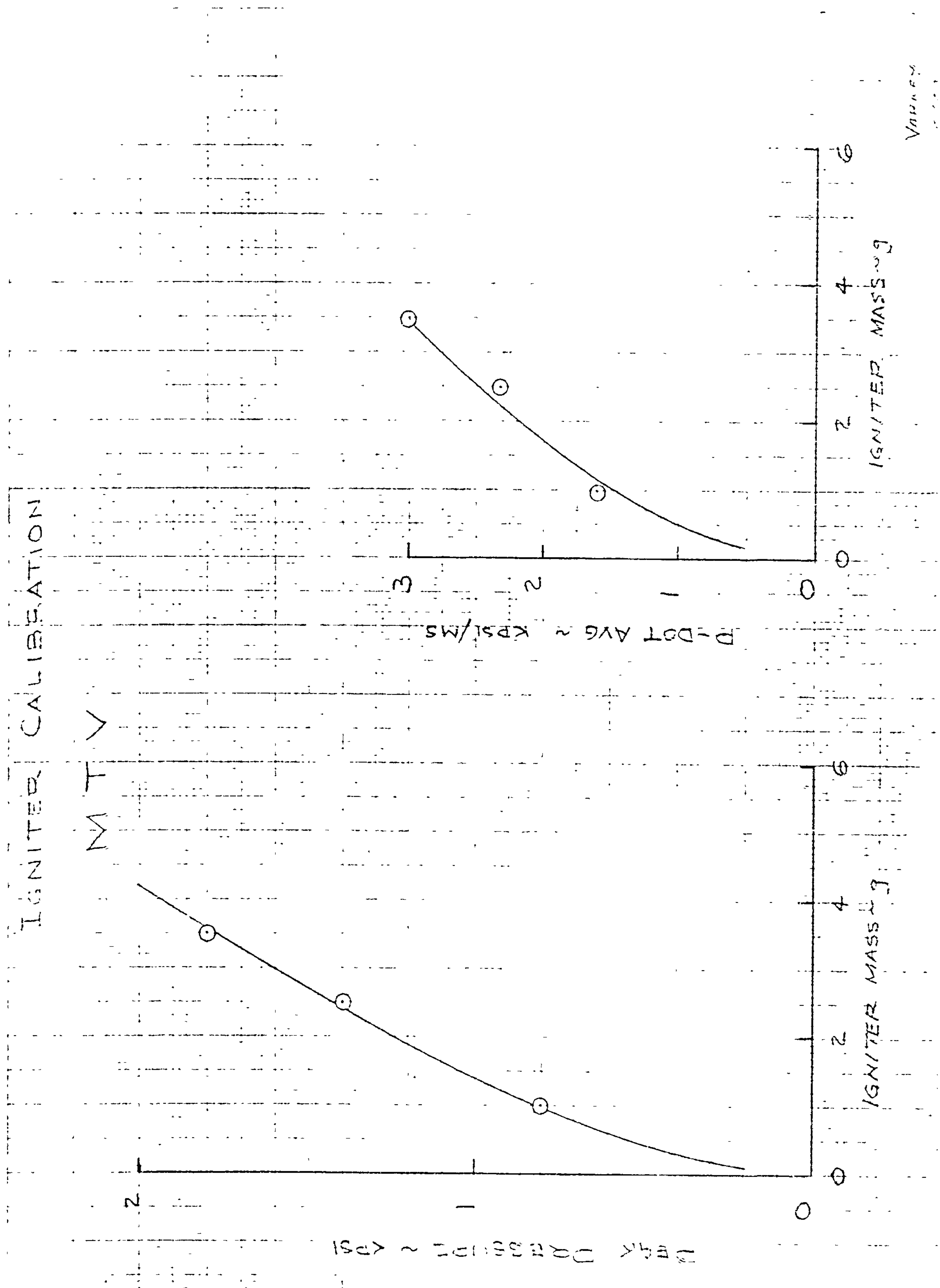

Figure D-4 Igniter Calibration Data: MTV

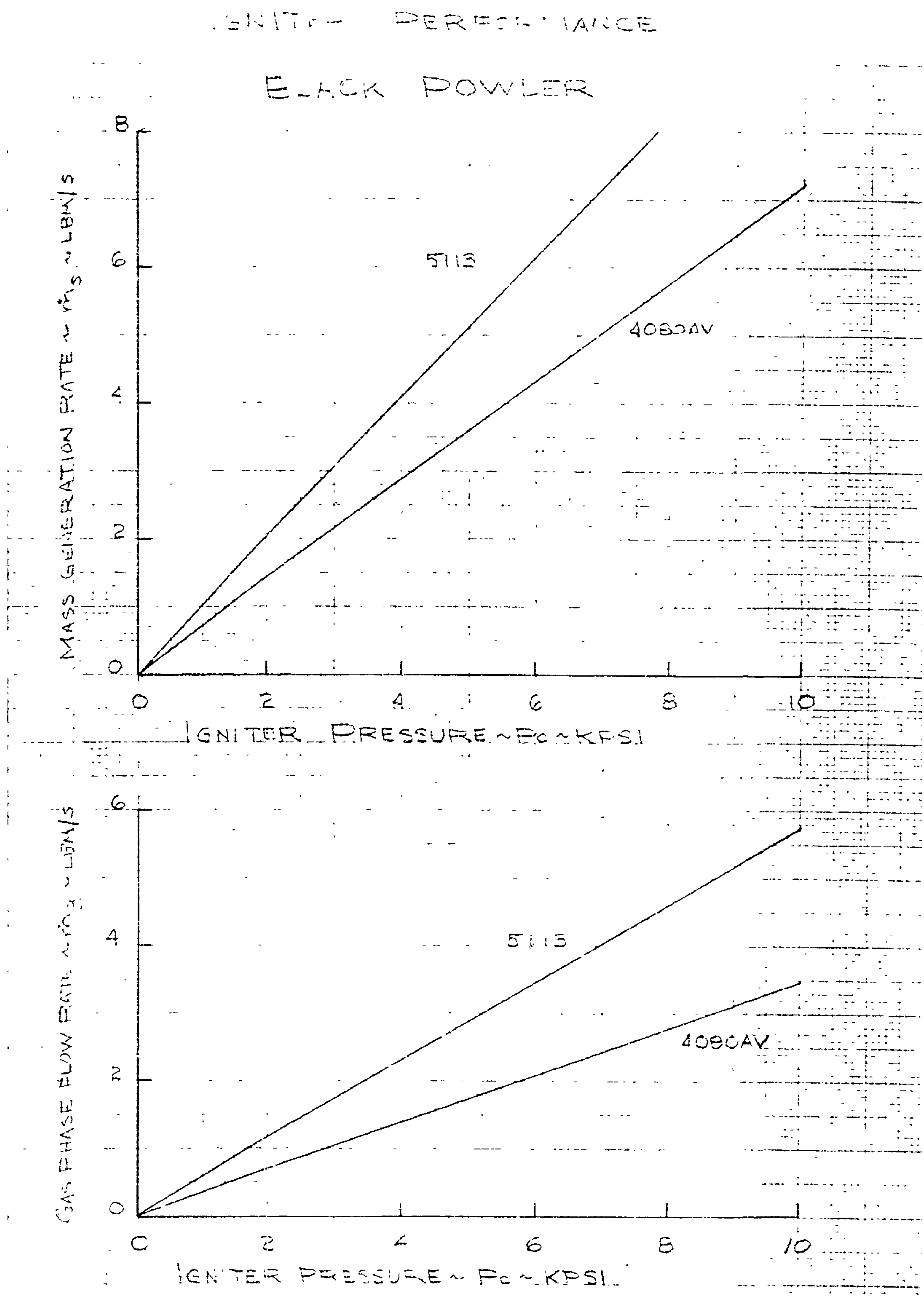

VARNEY 8/82

Figure D-5 Calculated Igniter Performance Characteristics: BP

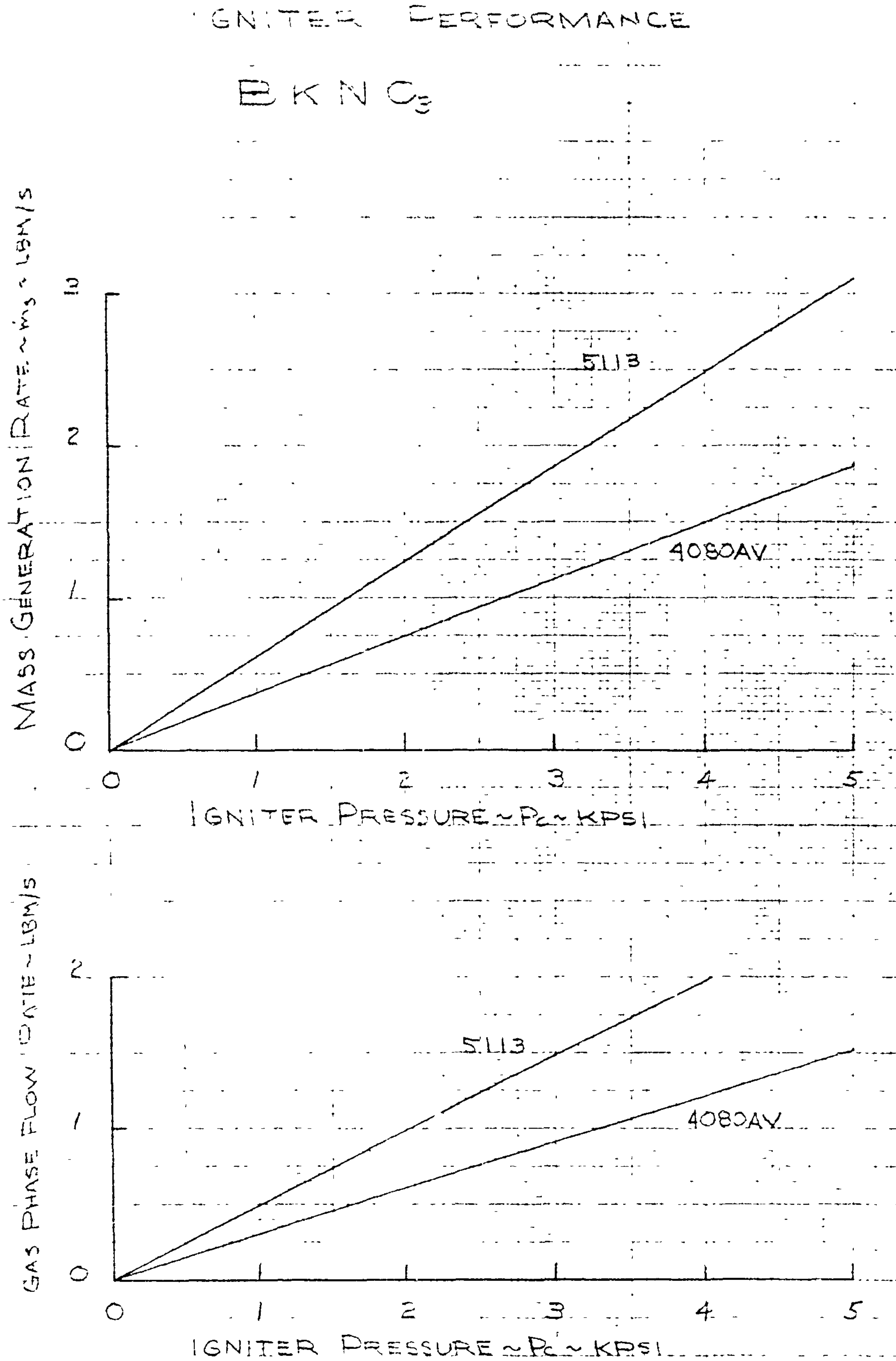

Figure D-6 Calculated Igniter Performance Characteristics: $BKNO_3$

VARNEY
8/82

IGNITER PERFORMANCE

NC

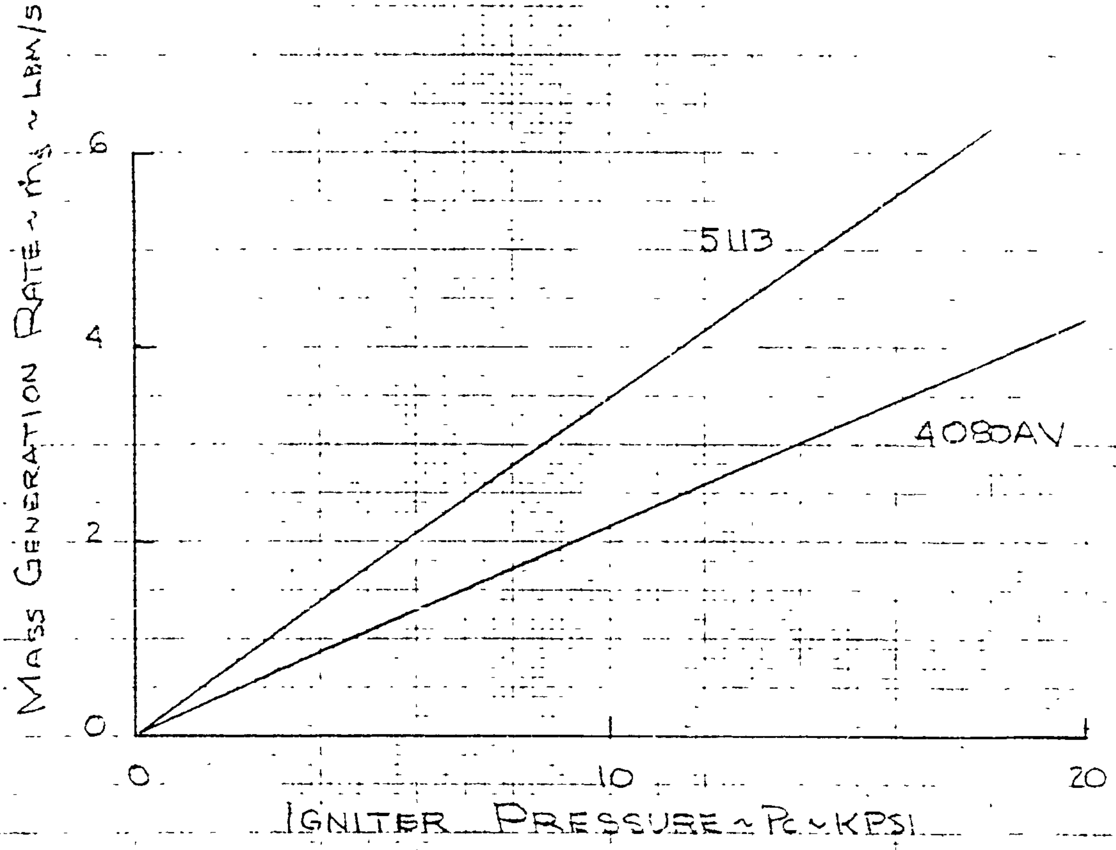

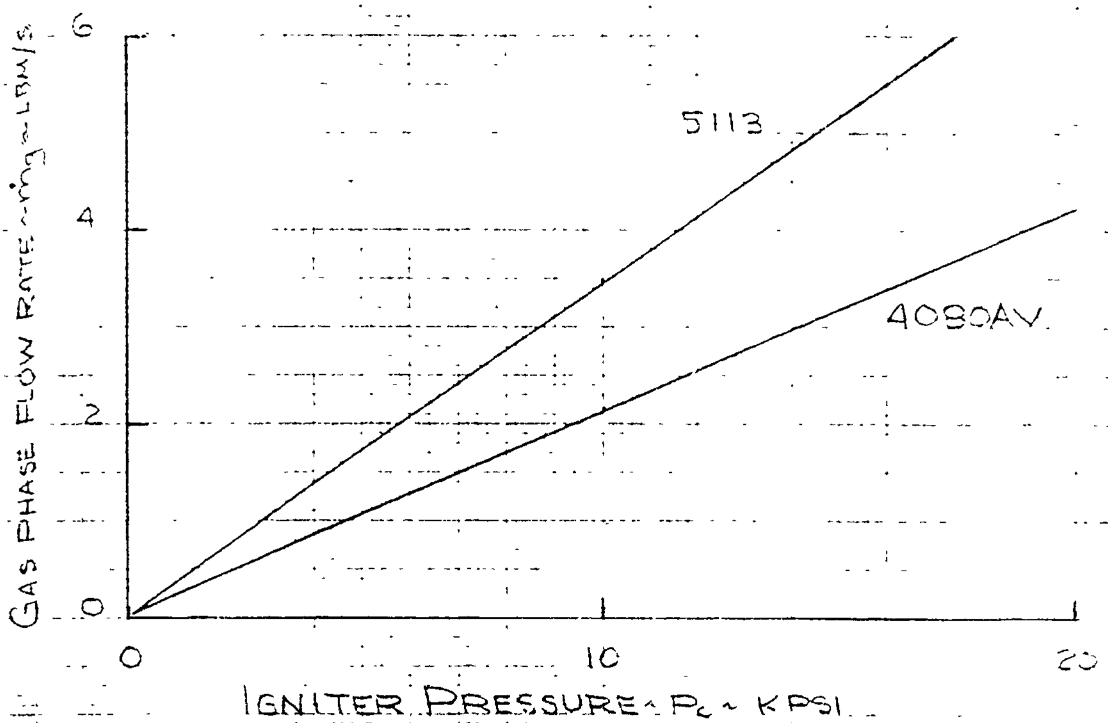

Figure D-7 Calculated Igniter Performance Characteristics: NC

IGNITER PERFORMANCE

MTV

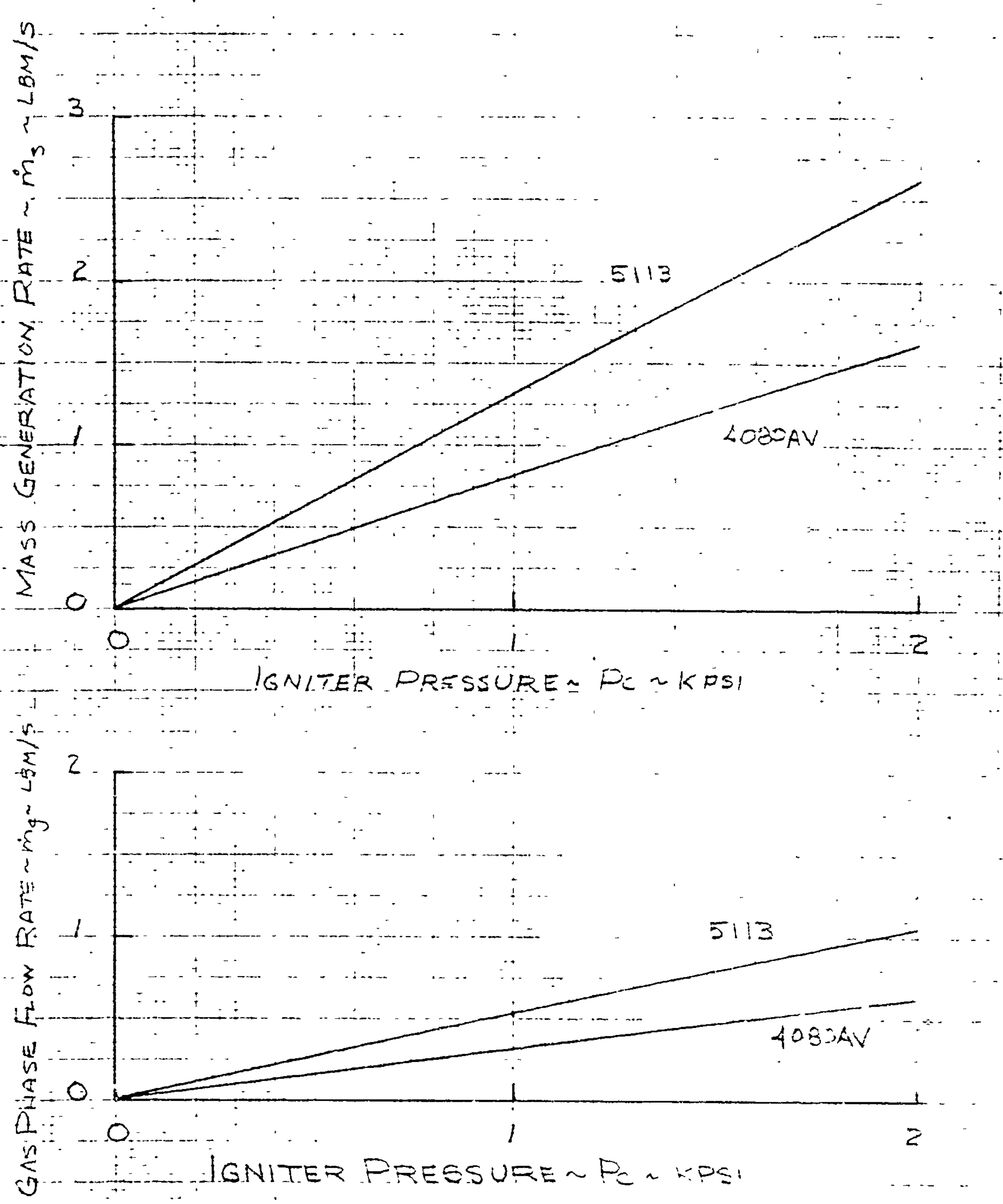

Figure D-8 Calculated Igniter Performance Characteristics: MTV

VARNEY
5/82

IGNITER PERFORMANCE

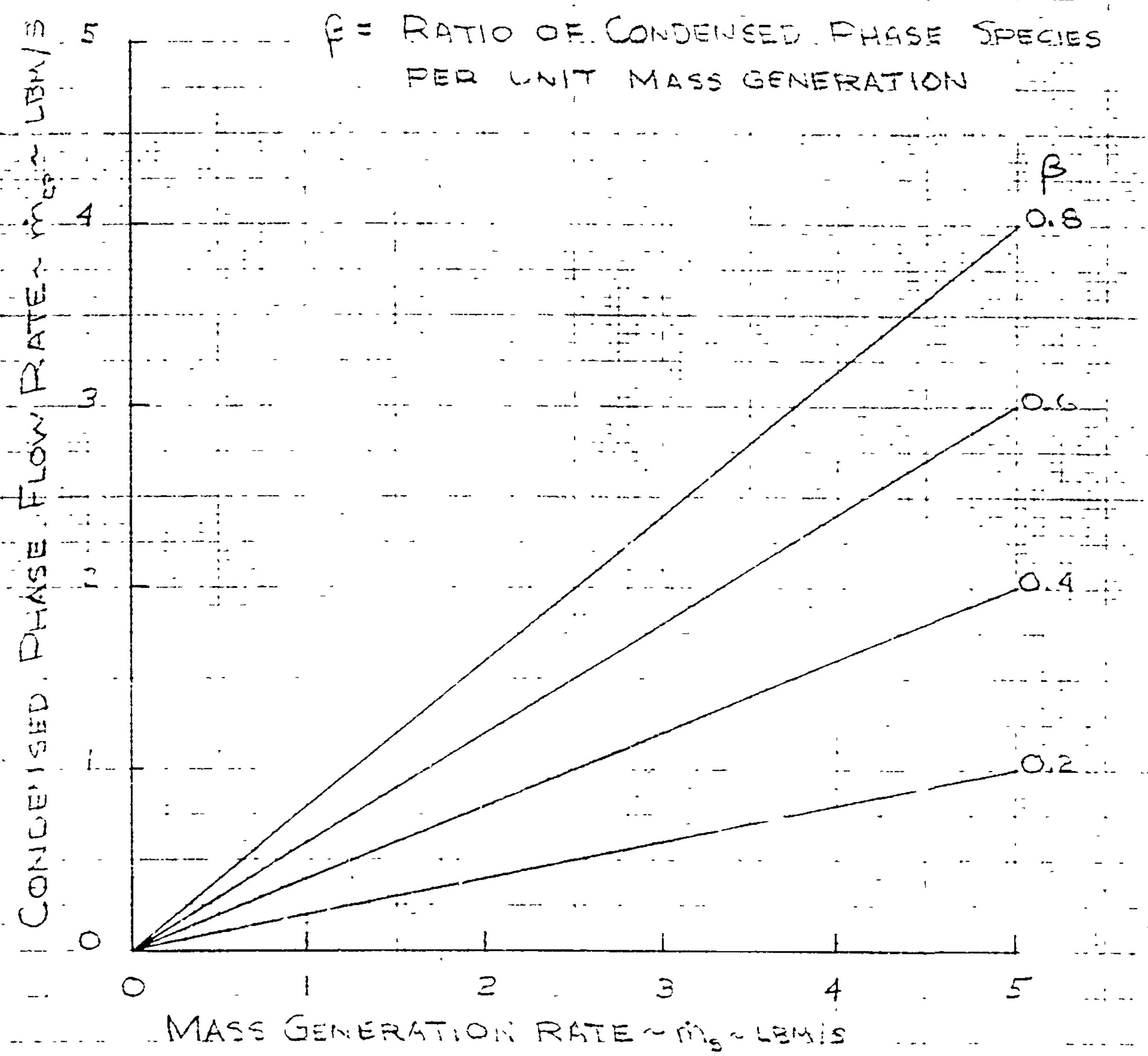

Figure D-9 Calculated Igniter Performance Characteristics: Condensed Phase Flow Rate

VARNEY
8/82

IGNITER PERFORMANCE

GAS PHASE ENERGY FLUX

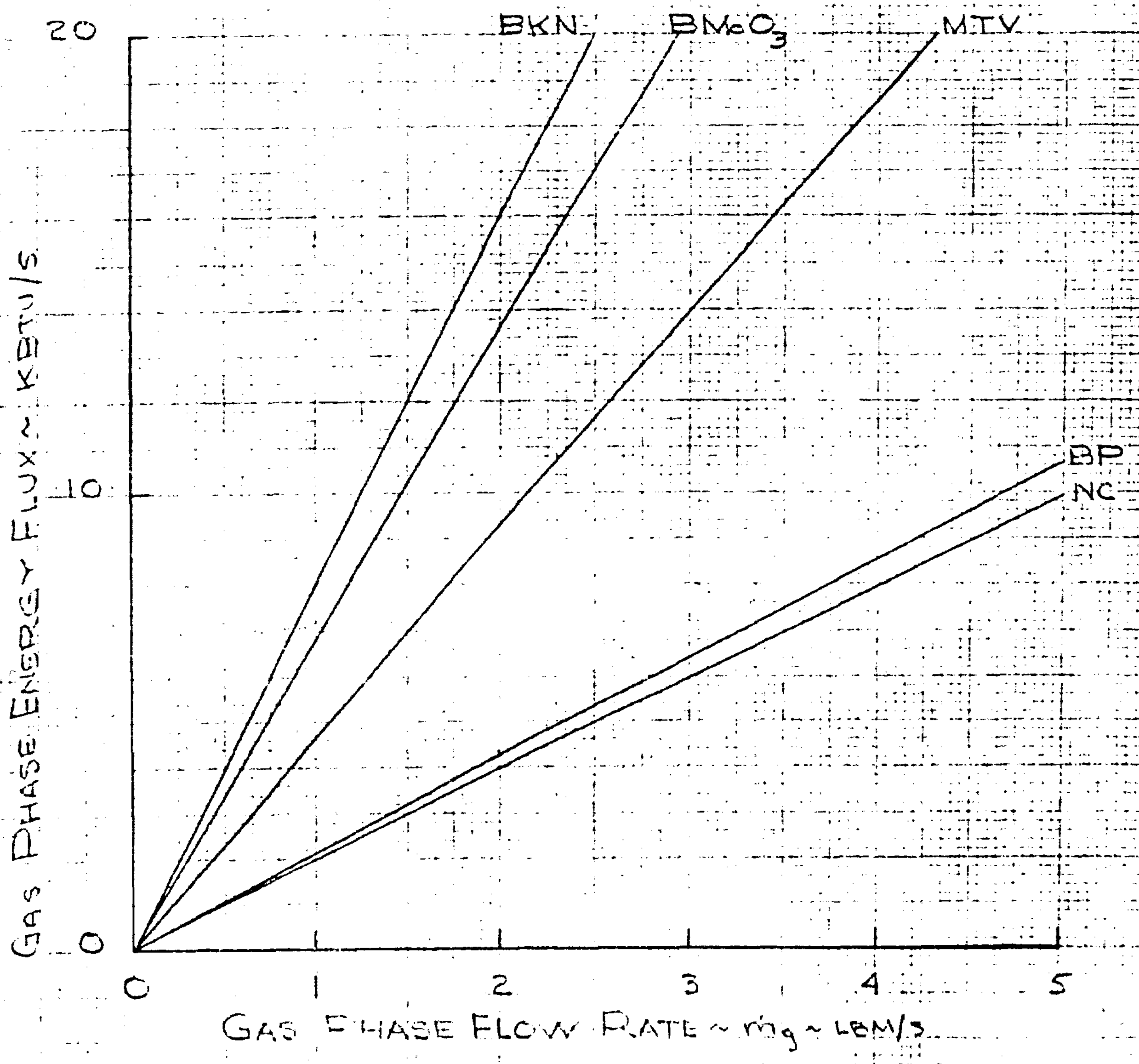

Figure D-10 Calculated Igniter Performance Characteristics: Gas Phase Energy Flux

VARNEY
8/82

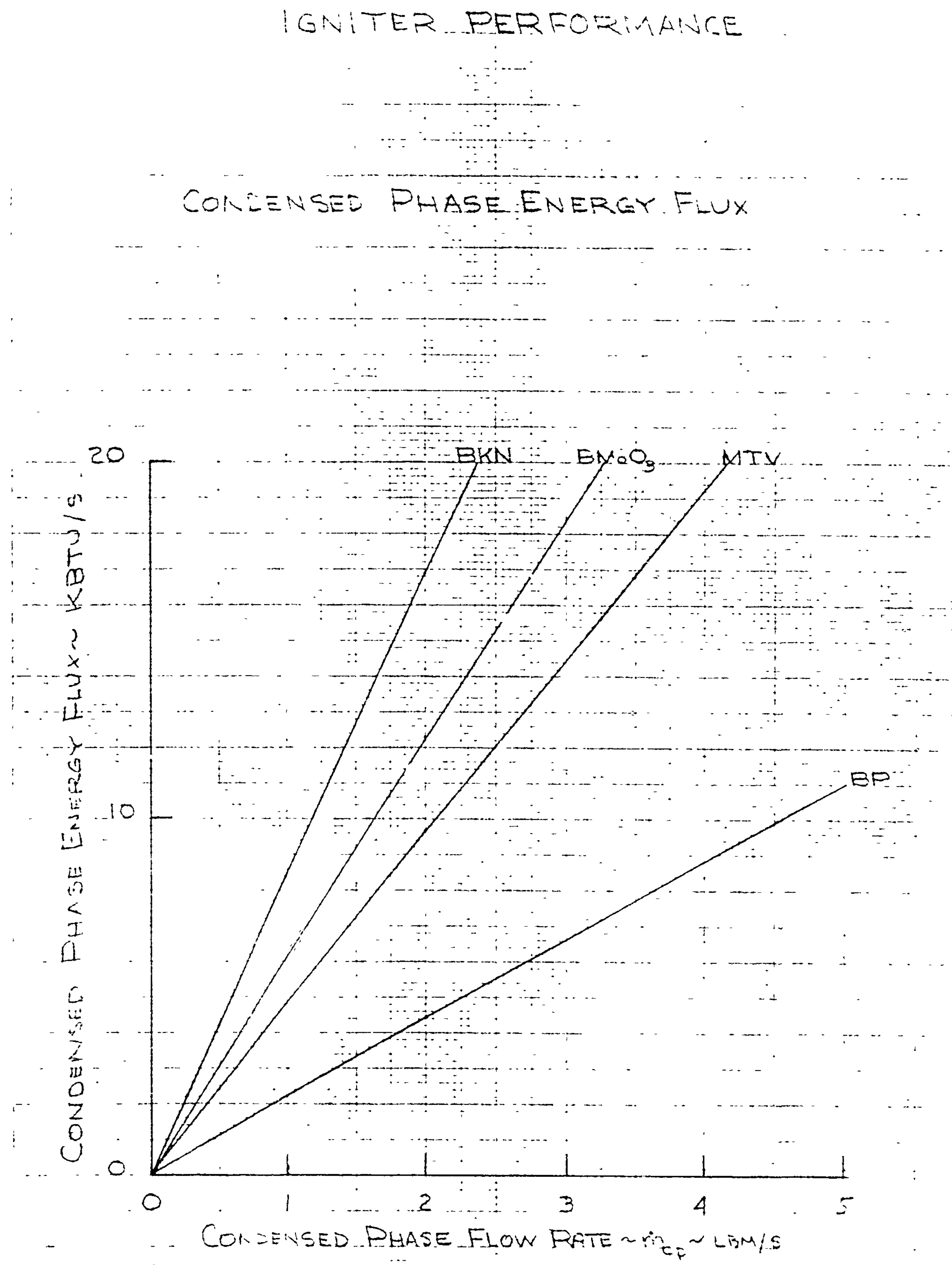

Figure D-11 Calculated Igniter Performance Characteristics: Condensed Phase Energy Flux

VARNEY
8/82

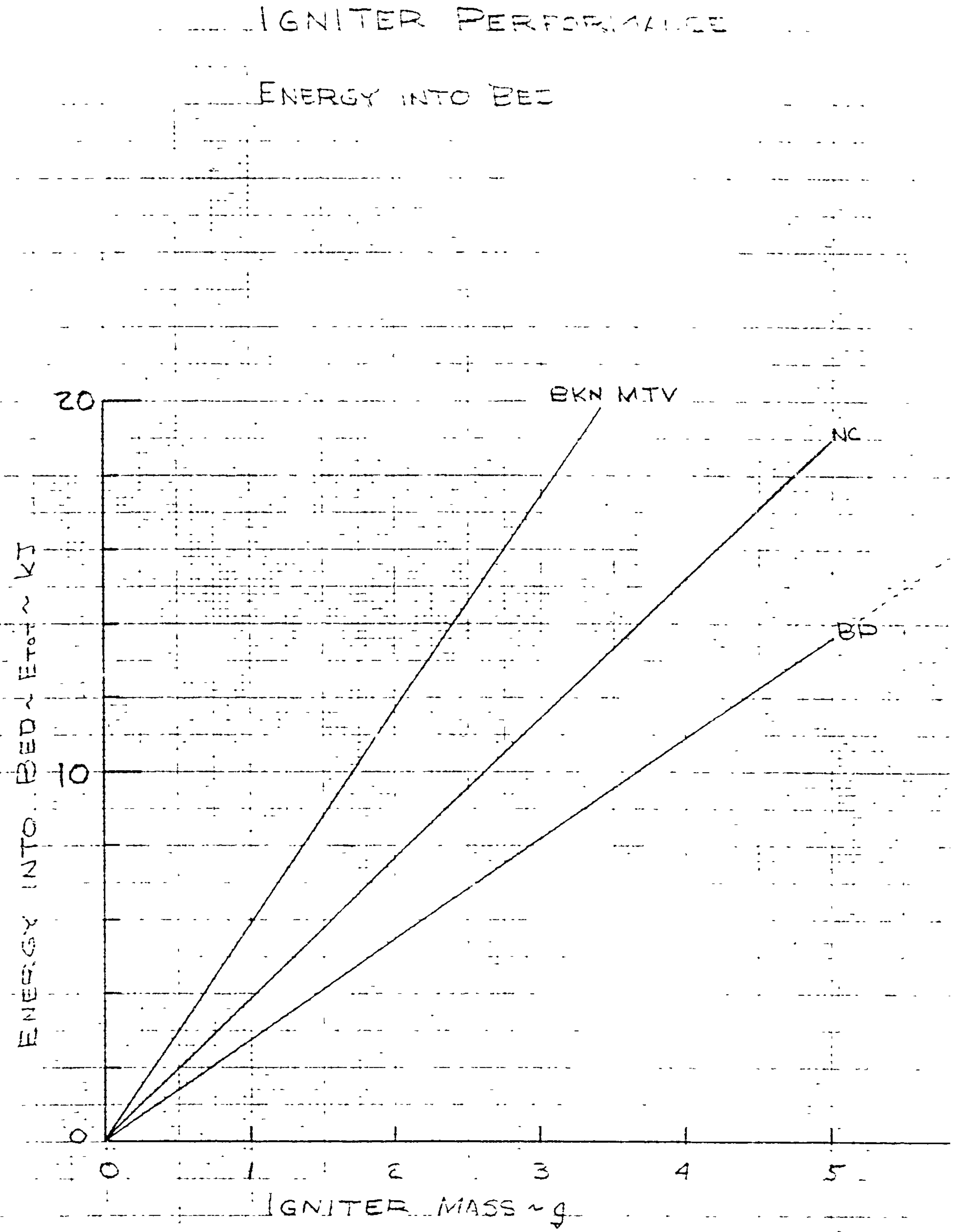

Figure D-12 Calculated Igniter Performance Characteristics: Total Energy into Bed

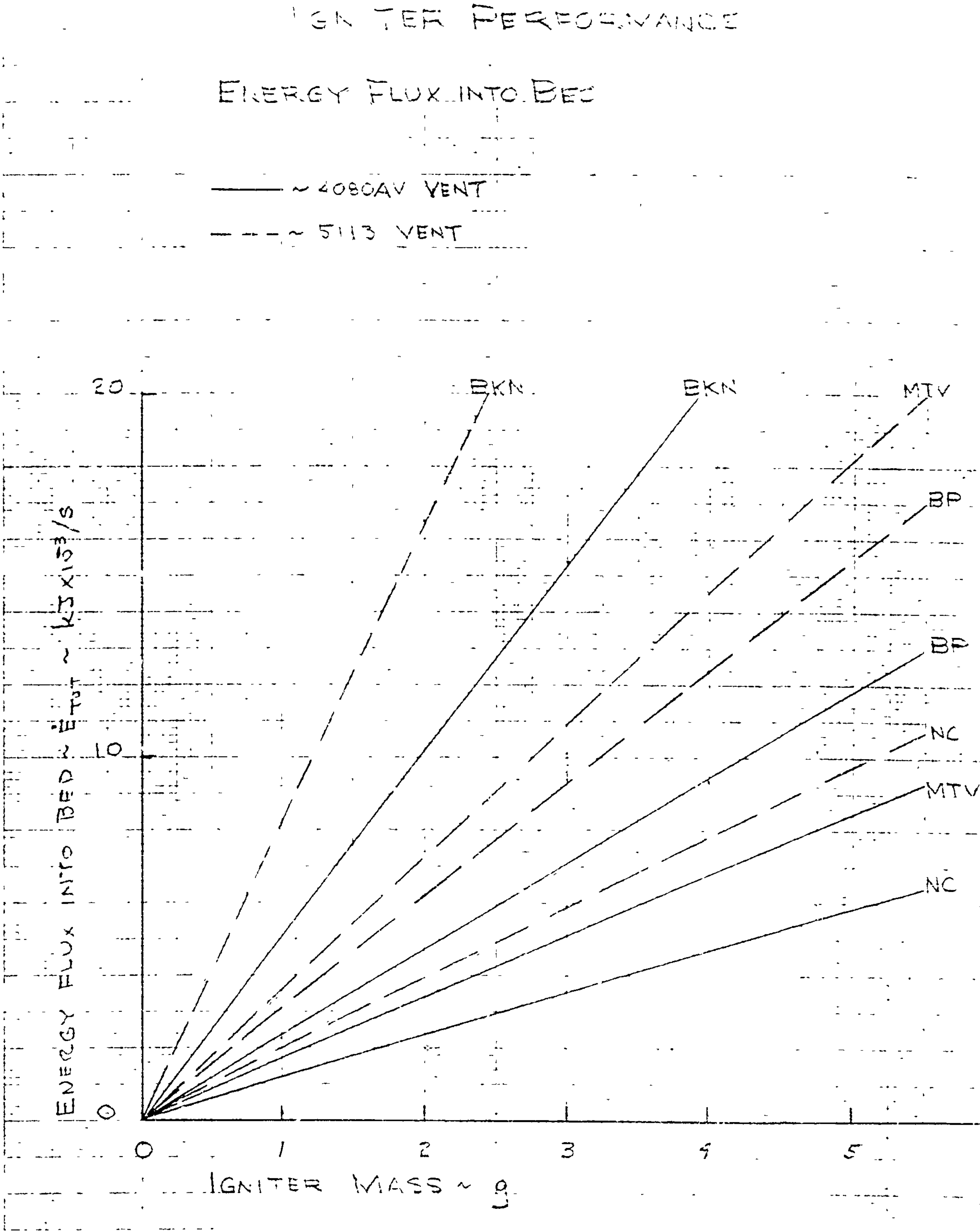

Figure D-13 Calculated Igniter Performance Characteristics: Energy Flux into Bed

VARNEY